NAIST-IS-DD1061032

Doctoral Dissertation

Studies on Interference Suppression Methods for ISDB-T in Fast Fading Channels

Ziji Ma

February 2, 2012

Department of Information Systems
Graduate School of Information Science
Nara Institute of Science and Technology

A Doctoral Dissertation
submitted to Graduate School of Information Science,
Nara Institute of Science and Technology
in partial fulfillment of the requirements for the degree of
Doctor of ENGINEERING

Ziji Ma

Thesis Committee:

Professor Mimoru Okada	(Supervisor)
Professor Hiroyuki Seki	(Co-supervisor)
Professor Kenji Sugimoto	(Co-supervisor)

Studies on Interference Suppression Methods for ISDB-T in Fast Fading Channels*

Ziji Ma

Abstract

As we all know, the conventional analog television broadcasting in Japan has entirely been replaced by DTV broadcasting that adopts the ISDB-T (Integrated Services Digital Broadcasting for Terrestrial) standard. BST-OFDM (Band Segmented Transmission-Orthogonal Frequency Division Multiplexing), as a primary modulation technique, has been adopted by the ISDB-T standard for its high frequency spectral efficiency and robustness against multi-path attenuation. With the spread of Digital Television (DTV), more and more attention is transferring from necessity to quality of DTV. In addition, the portable reception of DTV obtains the same, even more in quantity, attraction as the fixed reception. However, not like the conventional fixed reception, the mobile channel is more complicated due to the time-varying channel environment, and the portable reception also becomes more difficult to achieve the same receiving quality as the traditional television at home. A high-speed moving portable reception can be regarded as an ISDB-T receiver in fast fading channels where the main channel state information (CSI) is time-varying. And in the fast fading channels, the orthogonality between subcarriers of OFDM signal becomes easy to be destroyed, which will cause serious performance degradation to the ISDB-T reception. We focus on solving two most significant interferences, impulsive noise and ICI (Inter-Carrier Interference).

In order to suppress the interference from impulsive noise, a joint frequency-domain/time-domain scheme using adaptive parameters is proposed. The impact

*Doctoral Dissertation, Department of Information Systems, Graduate School of Information Science, Nara Institute of Science and Technology, NAIST-IS-DD1061032, February 2, 2012.

of impulsive noise can be detected by using the guard band in the frequency domain; meanwhile the main information of impulsive noise, including burst duration, instantaneous power and arrived time, can be estimated as well. Then a time-domain window function with adaptive parameters, which are decided in terms of the estimated position information of the impulsive noise and the carrier-to-noise ratio (CNR), is employed to suppress the impulsive interference. Simulation results confirm the validity of the proposed scheme, which improves the bit error rate (BER) performance for the ISDB-T receivers in both AWGN channel and Rayleigh fading channel.

For another serious interference for ISDB-T in fast fading channels, the ICI destroys the orthogonality between the subcarriers of OFDM signals, which will cause attenuation on system performance. We introduce a new compressed sensing method that can be used to estimate the channel state information (CSI) with very limited pilot tones. And then, an iterative equalization method named Parallel Interference Cancellation (PIC) using CS based channel estimation is introduced to compensate the OFDM signal suffered from the ICI for ISDB-T receivers. Computer simulation has been conducted, and it is clearly shown that the proposed method can effectively improve the BER performance of OFDM systems, in comparison with the conventional Least Square (LS) methods.

Keywords:

OFDM, ISDB-T, impulsive noise, channel estimation, fast fading, compressed sensing

Contents

List of Figures

List of Tables

Chapter 1

Introduction

1. Research Background and Objectives

Since the invention of television, people have been entirely attracted by the "magic" box that is the most popular home appliance in the world. There were over 1.4 billion television sets and 4.9 billion television audience in the world at the end of 2009, according to the statistic data from the International Telecommunications Union (ITU). Through television, we obtain much more information and happiness than conventional media, such as, newspaper and radio, and we also spend much time on watching TV. With the development of science and technology, television and broadcasting has experienced some important "innovation", from black and white to color, from analog to digital, from fixed indoor to mobile. Especially, the latest developing wave of digitization updating the analog equipment to digital is currently ongoing revolution around the world. Undoubtedly, the transition procedure will create a booming business market for equipment industries, research institutes and consumers. The DTV (Digital Tele-Vision) standards is a generalized conception, including terrestrial DTV, satellite DTV, cable DTV, even Internet Protocol TV (IPTV). In this thesis, we focus on the terrestrial DTV systems[1][2].

Reviewing the development of Digital Terrestrial Television Broadcasting (DTTB), three DTV standards have proceeded in parallel in Japan, Europe and United States, respectively. They all have various technique route, political background, and applicable region. Also they have different advantages and shortcomings.

It is difficult to draw an easy conclusion which one is better. As a comparison between them, the main parameters and features of three systems are shown in Table.1.1.

The ASTC (Advanced Television Systems Committee) standard was firstly proposed in 1982 by the member organizations of the Joint Committee on Inter-Society Coordination (JCIC). It was also firstly adopted for business in 1996 in the USA. Originally, the ASTC was designed for replacing the traditional analog systems but not abandoning the conventional equipments. It is the unique single carrier standard that does not adopt multi-carrier modulation technique, but using 8-level Vestigial-Sideband (VSB) or 16-VSB. The information bit rate for ATSC is up to 19.39Mbit/s in 6MHz terrestrial channel [3].

The European standard, DVB-T (Digital Video Broadcasting for Terrestrial), is the so-called "most popular" one that is adopted most widely, not only in Europe, but Africa, Asia, Oceania [4]. It was standardized in 1997, and firstly started for service in the United Kingdom in 1998. It was developed for 8MHz bandwidth channels, and can be adjusted into 6, 7 or 8MHz to match TV frequency plans in various countries. It employs a multi-carrier modulation technique, namely COFDM (Coded Orthogonal Frequency Division multiplexing). The achievable bit rate in 8MHz channel ranges from 4.98Mbit/s to 31.67Mbit/s. It has two operational modes: "2k mode" for 2k FFT (Fast Fourier Transform) and "8k mode" for 8k FFT. Moreover, in comparison with ATSC, DVB-T is more flexible to change its transmission parameters, including modulation type, code rate, length of guard interval (GI), etc, to adapt various environments. If channel environment is relatively "clean", DVB-T systems will use high-speed model by adjusting the transmission parameters [1]. Certainly, more flexibility results in more complicated system's architecture.

The Association of Radio Industries and Businesses (ARIB) in Japan developed the third major standard, ISDB-T (Integrated Services Digital Broadcasting for Terrestrial). It is the most complicated one among three standards, in order to obtain enough flexibility to deliver digital television and sound programs, and offer various types of multimedia services, such as video, audio, text and computer programs, will be integrated. In particular, it has been designed with a one-segment mode in the center of bandwidth for portable receivers or mobile phone.

Table 1.1. Characteics of three DTTB systems

System	**ATSC[3]**	**DVB-T[4]**	**ISDB-T[5]**
Adopted Region (mainly)	North America	Europe & Oceania & North Africa & South Asia	Japan & South America
Source Code			
Video	Main profile syntax of ISO/IEC 13818-2 (MPGE-2 video)		
Audio	ATSC standard (Dolby AC-3)	MPEG-2 and Dolby AC-3	MPEG-2-AAC
Transport stream	ISO/IEC 13818-1 (MPEG-2 TS) transport stream		
Channel coding			
Outer coding	RS(207,187, t=10)	RS(204,188, t=8)	
Outer interleaving	52 RS block interleaving	12 RS block interleaving	
Inner coding	Rate 2/3 trellis code	Punctured convolutional code	
Inner interleaving	12:1 Trellis interleaving	bit-wise interleaving and frequency interleaving	bit-wise interleaving, frequency interleaving, selectable time interleaving
Data randomization	16bit PRBS[a]		
Modulation	8-VSB[b] for Terrestrial mode and 16-VSB for cable mode	COFDM	BST-OFDM with 13 frequency segments
Modulation type		QPSK, 16QAM, and 64QAM	DPSK, QPSK, 16QAM, 64QAM

[a]Pseudo Random Binary Sequence
[b]Vestigial Side Band

Similar to DVB-T standard, the ISDB-T employs a multi-carrier modulation method named Band Segmented Transmission (BST) OFDM, which consists of a set of common basic frequency blocks called BST-Segments [5]. We will describe and discuss this standard in detail in the next section.

However, in China, which as one country has the largest number of television watchers in the world, the developing route and current situation of DTTB is very complicated [6]. About 10 year ago, DVB standard had a very hopeful chance to enter the Chinese market, and some DVB mobile televisions have even been equiped and adopted by some public bus systems in several Chinese cities [7]. But the enormous patent fee for DVD techniques that Chinese manufacture had paid gave Chinese government a lesson that using other countries' patents was very expensive. Therefore, Chinese government hopes to develop another DTTB standard themselves. So did the Chinese 3G mobile standard. However, till now, the argument between DTMB (Digital Terrestrial Multimedia Broadcasting) and CMMB (China Mobile Multimedia Broadcasting), as two main standards, still continues [8][9]. Choosing which one as future Chinese DTV standard has becosme a competition within different official departments rather than comparison on system performance.

Nowadays people are not content with just sitting in sofa, drinking cola and watching laughable talking show in the front of television, as well. The consumers ask for more, like high definition, 3 dimension, inter-activity, etc. They hope to watch high definition TV anytime, anywhere, even in a fast moving automobile. Fortunately, it is not an unrealizable dream, DTV broadcasting techniques can help us to realize it. Moreover, people will be more satisfied and enjoy better, if we are capable to suppress the interference from which television suffers in fast fading channels. However, many practical troubles, like multi-path propagation, time-various channel, impulsive noise, etc, which exist, usually one kind or several kinds of them in fast fading channels, make the high definition DTV become difficulty to keep robust reception to the degraded signal. Certainly, OFDM technique can help DTV receivers to overcome multi-path propagation to some extent, and time interleaving and frequency interleaving is also effective against impulsive noise to improve system bit error rate (BER) performance. However, practical measure results demonstrate that the currently adopted techniques can-

not entirely suppress the interference in fast fading channels [10][11]. Therefore we concentrated on resolving two of the most significant problems in fast fading channels,

- Interference due to impulsive noise.
- Inter-Carrier Interference (ICI).

The impact of impulsive noise for DTV is very significant. Someone may have the experience of living in a hotel besides an airport. Whenever an airplanes takes off or lands, the screen of television will appear some abnormal activities, which is just the effect from the impulsive noise. The impulsive noise may come from engines, home appliances, thunderbolt, or something else. In fast fading channel, the interference of impulsive noise is also a serious problem with which we have to be faced.

In fast fading channels, the channel state information (CSI) is time-varying, thus the channel estimation is more difficult than in flat fading channels. Being a precondition of demodulation, reconstruction of CSI by channel estimation is necessary. Generally, the pilot-assisted methods are widely adopted for channel estimation, which insert some pilot tones into OFDM symbols as training sequence at transmitter and estimate the CSI from the extracted pilot tones at receivers [12][13]. However the pilot tones occupy some data sub-carriers and decrease the spectral efficiency. In general, the more complicated the channel is, the more pilot tones need to be inserted. Therefore, a new channel estimation approach with balance between estimation accuracy and spectral efficiency becomes one of our research objectives. After that, some equalizers are employed to suppress the ICI. If ICI is not adequately compensated, the ICI will result in an error floor. And the one-tap equalizer with reasonable performance in flat fading channels is not necessarily satisfactory in fast fading channels. Therefore, we also concentrate on developing an equalizer to mitigate ICI in fast fading channels.

2. Organization

The rest of this thesis is organized as follows. Chapter 2 describes the ISDB-T standard in detail, and the OFDM systems. Chapter 3 presents several well-

known models of impulsive noise and analyzes the impact of impulsive noise for ISDB-T receivers. In Chapter 4, an adaptive scheme of impulsive noise suppression is introduced that combines frequency-domain detection and time-domain suppression to achieve a sub-optimized balance between efficiency and performance. A Compressed Sensing (CS) based equalizer for fast fading channel is then introduced in Chapter 5. As a new methodology, CS is employed to complete channel estimation with less pilot tones and more accurate reconstruction. In Chapter 6, we summarize our research work. In terms of the successful and failure experience that happened during this work, we simply present some future work and open questions which may be helpful to someone who is interested in this research field.

Chapter 2

ISDB-T: Integrated Services Digital Broadcasting for Terrestrial

1. Introduction

This chapter gives an overview of the ISDB-T standard. DTV broadcasting supported by ISDB-T standard has started on service in Japan since December 2003, and the conventional analog broadcasting has already been stopped since July 2011. ISDB-T is the most complicated and flexible standard among three major DTV standards, and provides very abundant digital broadcasting services, such as HDTV (high-definition TV), SDTV (standard-definition TV), sound, graphics, text, etc. The main characters of ISDB-T standard include[5]:

- One transmission channel provides one high-definition DTV program or three standard-definition DTV programs.
- It is available to provide SDTV, sound, data, etc, to moving receivers, such as, vehicles, buses, and so on.
- Signals for fixed and mobile receivers can be combined in transmission by means of the hierarchical layers.

- The center segment of bandwidth can be independently transmitted as audio and data services for partial reception by portable receivers.
- ISDB-T is claimed to have robustness to multipath interference, co-channel analog television interference, and so on.
- ISDB-T can be received indoors with a simple indoor antenna.
- ISDB-T provides good expansibility and quite flexibility for various transmission environments.

2. OFDM: Orthogonal Frequency Division Multiplexing

Orthogonal Frequency Division Multiplexing (OFDM) was firstly proposed to use parallel data and frequency division multiplexing with overlapping sub-channels to avoid the use of high-speed equalization and to combat multipath distortion and impulsive noise in 1970's in the USA [14]. Now it is becoming widely applied in various communication systems due to its high rate transmission capability with high bandwidth efficiency and its robustness with regard to multi-path fading and delay. It has been adopted in many popular communication standards, such as WLAN (Wireless Local Area Network), WiMAX (World Interoperability for Microwave Access), DVB, DSL (Digital Subscriber Line), PLC (Power Line Communication), and ISDB-T. In contrast with the single-carrier system, OFDM is classified as a multi-carrier system, which modulates the orginal mapped data sequence onto orthogonal sub-carriers and transmits the modulated symbols in parallel. In multi-carrier transmission systems, the available bandwidth is divided into N orthogonal sub-channels. Different symbol sequences are sent in parallel using the divided orthogonal sub-channels, as shown in Fig. 2.1.

2.1 Modulation Model of OFDM

The block diagram of typical OFDM transmitter and receirver are respectively shown in Fig. 2.2 and 2.3. OFDM is a parallel transmission system in which

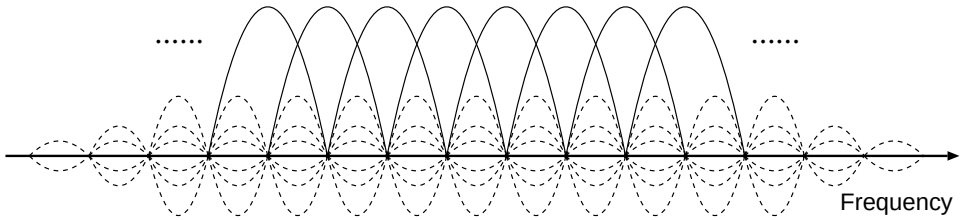

Figure 2.1. Spectrum construction of OFDM symbol (orthogonal sub-carriers)

several sequential streams of data are transmitted simultaneously. So it is very important to notice that Discrete Fourier Transform (DFT) and Inverse Discrete Fourier Transform (IDFT), which is usually conducted be means of Fast Fourier Transform (FFT) and Inverse Fast Fourier Transform (IFFT), is the primary process that accomplish the modulation and demodulation for parallel data. The IFFT block transforms the data sequence into time domain, and then a guard interval (GI) is inserted between OFDM symbols. After A/D and transmission terminal, the signal is transmitted and passed through wireless channel. At the receiver, GI is first removed from received signal, and then the FFT block is used to transform the date back to frequency domain. The output of FFT is fed to the next equalizer, demodulator and decoder.

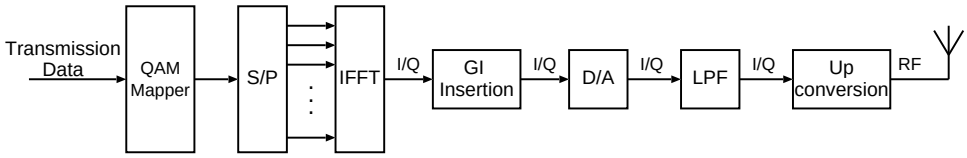

Figure 2.2. OFDM transmitter

2.2 Guard Interval

Another important feature of OFDM system is the insertion of Guard Interval (GI) that is inserted into two OFDM symbols to avoid Inter-Symbol Interference

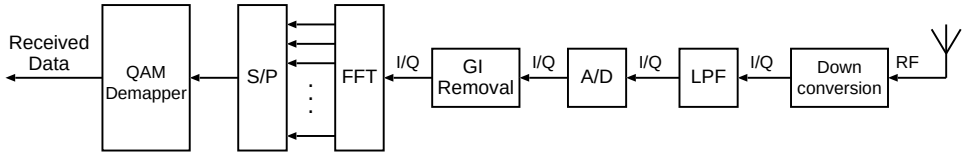

Figure 2.3. OFDM receiver

(ISI) due to multi-path delaying propagation [15]. And GI is removed at the receivers before FFT. In order to entirely avoid ISI and Inter-Carrier Interference (ICI), the length of GI, in theory, should be at least as long as the channel impulse response. The practical length of GI is application-dependent. There are two well-known GI types, Zero padded (ZP) and Cyclic Prefix (CP). The former is made of a sequence of zeros, while the latter is a copy of the OFDM symbol's tail part. Generally, the CP is more often adopted as GI, since it can help the system to keep carrier synchronization and is easy to model the transmission system as cyclic convolution. The basic affect of CP as a GI is shown in Fig. 2.4.

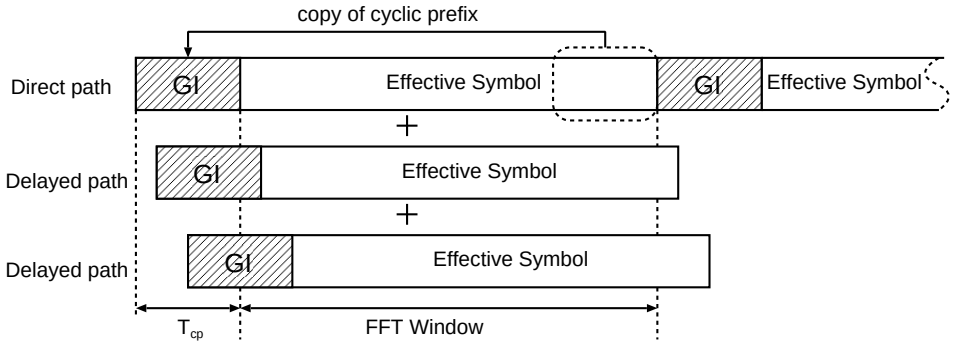

Figure 2.4. Guard interval and its effect

2.3 Advantages of OFDM

In contrast with single-carrier system, the advantages of OFDM are mainly shown as following,

- OFDM system has better spectral efficiency, because the structure of orthogonal sub-carriers is very dense to save the spectrum. While single-

carrier system has to insert more guard bands into adjacent channels.

- OFDM system can more simply overcome ISI by using GI, however it is necessary for a single-carrier system to employ more complex equalization.
- OFDM system has more flexibility by adjusting its main parameters depending on the transmission environment.
- OFDM system shows more tolerate against narrow band, because only part of sub-carriers suffer from interference.

3. General Features

The effective bandwidth of one ISDB-T channel is allocated to 5.57MHz to match the existing analog television systems, and the total bandwidth is separated to 13 segments, each of which has 430kHz. And the transmission parameters of ISDB-T can be independently applied for each segment. In terms of the different services, ISDB-T standard selects different segments for transmission. In addition, the transmission parameters of ISDB-T can be independently applied for each segment. For example, for HDTV, all 13 segments are used for enlarging transmission capacity, while for SDTV, using 4 segments is enough to achieve capacity requirement. Furthermore, the center segment within all 13 segments is in particular designed for mobile terminals with low bit-rate TV. The main parameters of ISDB-T standard are shown in Table. 2.1.

ISDB-T has three modes, mode1, mode2 and mode3, depending on the number of subcarriers, while its bandwidth is nearly the same as 5.6MHz with little difference. Mode1 is sensitive to multi-path delay spread for its short symbol duration, but it is more robust to Doppler shift than the other 2 modes for its wide sub-carrier interval. Alternatively, mode3 is robust to multi-path delay spread, but relatively not resistant to Doppler shift. Performance of mode2 is between that of mode1 and mode3. The main parameters of ISDB-T are decided depending on the channel environment. If the reception is stable with little interference, choosing high-array modulation type, efficient convolution code rate and short GI ratio can increase the information rate. On the contrary, in the case of instable channel suffered from numerous interference, the main adjustable parameters,

Table 2.1. Parameters of ISDB-T standard

Mode	**Mode1**	**Mode2**	**Mode3**
Frequency band	UHF & VHF 470MHz-770MHz (50 physical channels)		
OFDM segments	13		
Allocated bandwidth	6MHz (7MHz, 8MHz also available)		
Effective bandwidth	5.575MHz	5.573MHz	5.572MHz
Sub-carrier interval	3.968kHz	1.984kHz	0.992kHz
Effective symbol period	252μs	504μs	1008μs
FFT window size	2048	4096	8192
FFT sampling speed	512/63 = 8.12698 MHz		
Number of sub-carriers	1405	2809	5617
Number of data sub-carriers	1248	2496	4992
Sub-carrier modulation	QPSK, 16QAM, 64QAM, DQPSK		
Number of symbol per frame	204		
Inner coder	Convolution coder (code rate 1/2, 2/3, 3/4, 5/6, 7/8)		
Outer coder	Reed-Solomon (204, 188)		

modulation type, convolution code rate and GI ratio, have to be chosen to decrease the information rate but keep the ISDB-T reception stable and robust. This feature shows the ISDB-T standard's flexibility and adaptability.

4. Partial Reception

ISDB-T adopts a unique technique named partial reception to reduce receivers' power consumption. The most important factor to reduce power consumption is to decrease the signal processing speed in receivers. That is the reason why it can be easily and effectively adopted by mobile reception. In addition above, as for an OFDM segment at the center of 13 segments, it is possible to conduct channel coding such that the range of frequency interleaving is limited within the segment. This configuration enables an ISDB-T receiver to receive one-segment service embedded in a hierarchical television signal. As shown in Fig. 2.5, in case of partial reception, the center segment of 6MHz OFDM bandwidth is filtered by narrow band pass filter (BPF) whose pass band is 432 kHz. Output of narrow band filter is demodulated by low sample rate FFT whose sample rate is only 1/8 of high sample rate of FFT.

5. Multiplex and Channel Coding

The block diagram of ISDB-T transmitter is shown in Fig. 2.6 in detail. The receiver is the reverse process of the transmitter. With ISDB-T, one or more transport stream (TS) inputs, defined in "MPEG2" standards, are re-multiplexed to create a single TS. The TS is then subjected to multiple channel-coding steps in accordance with the intentions of the service, and is finally sent as a single OFDM signal. A re-multiplexed TS is formed by multiplex frames as elementary units, each of which consists of n pieces of transport-stream packets (TSP). Each of the TSPs comprising a multiplex frame is 204 bytes in length consisting of 188-byte program data and 16-byte null data. Table. 2.2 shows the numbers of TSPs used for different modes and GI ratios. Each of the transmission TSPs within a multiplex frame is transmitted by hierarchical layer (A, B or C) of an OFDM signal or belongs to a null packet ($\mathrm{TSP}_{\mathrm{null}}$) that is not transmitted as an

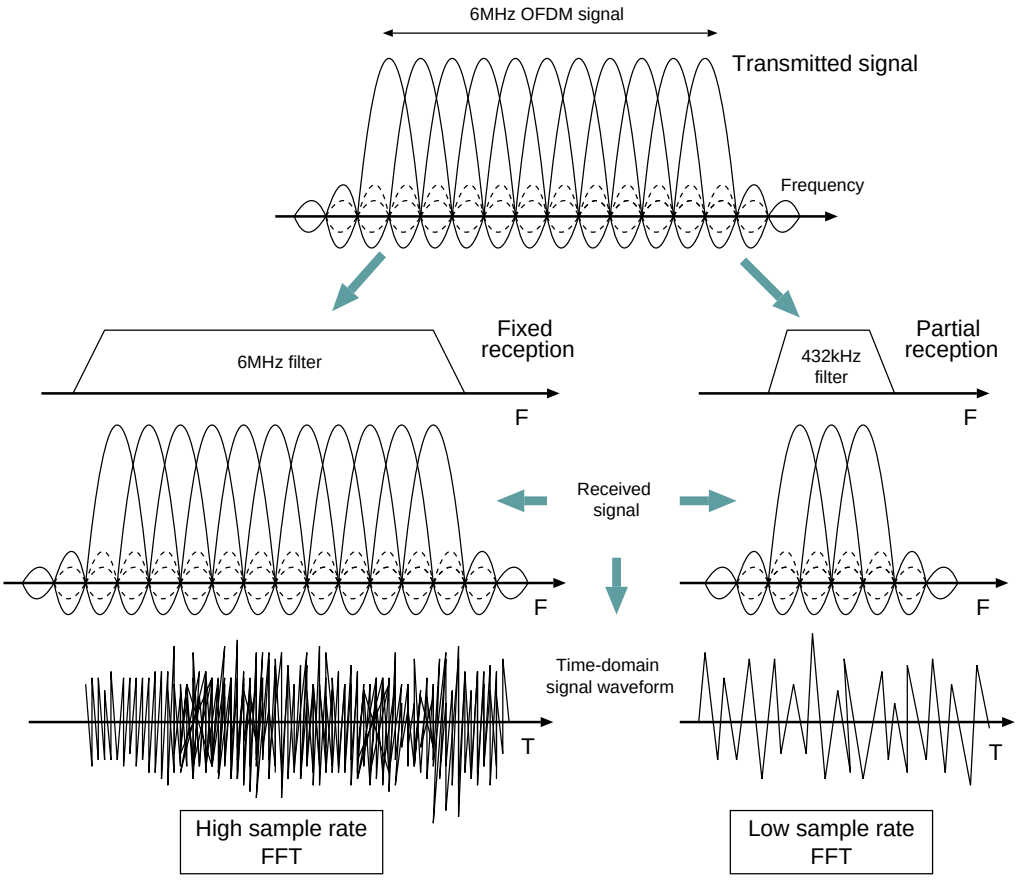

Figure 2.5. Partial reception and wideband reception

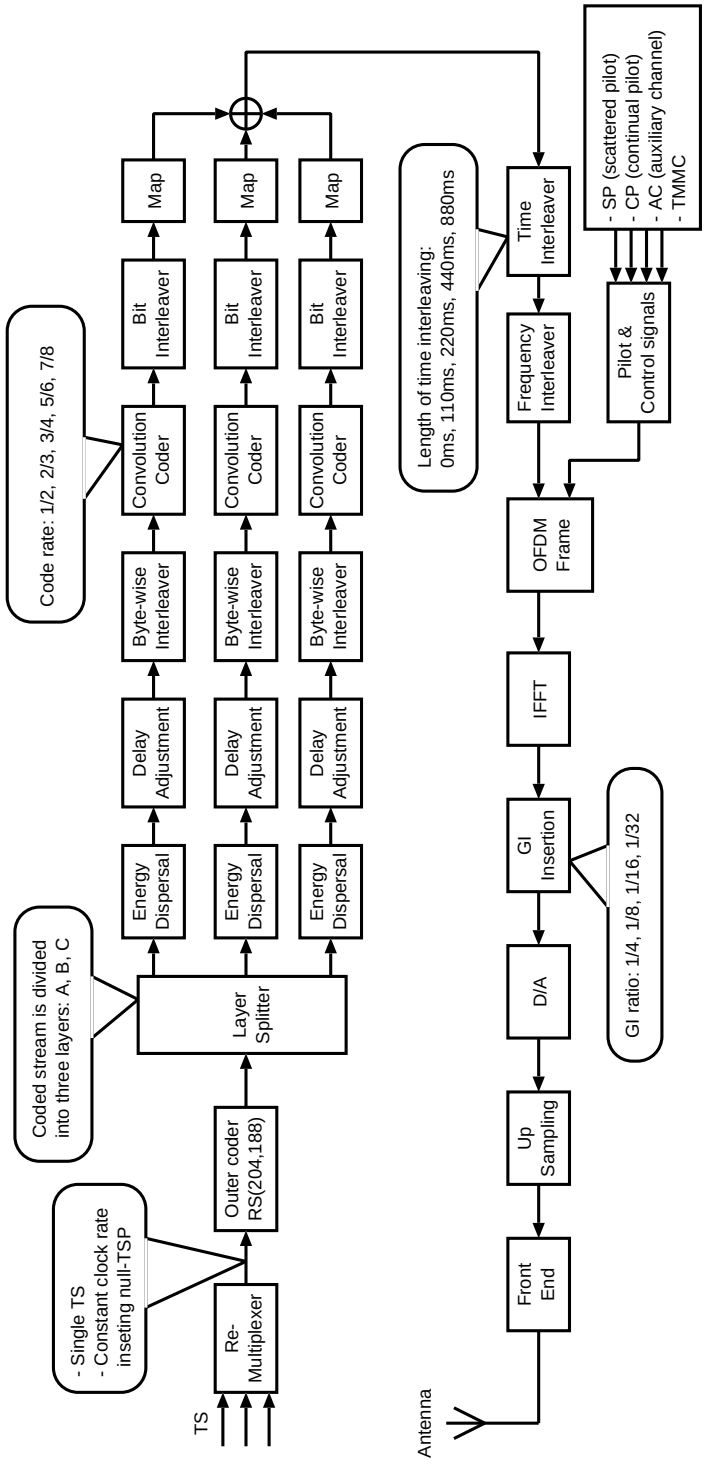

Figure 2.6. ISDB-T transmitter block diagram with source coder, channel coder, interleaver and BST-OFDM

OFDM signal.

Table 2.2. Parameters of ISDB-T standard

Mode	Number of transmission TSPs included in one multiplex frame			
	GI ratio 1/4	GI ratio 1/8	GI ratio 1/16	GI ratio 1/32
Mode1	1280	1152	1088	1056
Mode2	2560	2304	2176	2112
Mode3	5120	4608	4352	4224

After that, a shortened Reed-Solomon code (204, 188) is used in every TSP as an outer code. The inner coder after byte interleaving is introduced in advance. The inner code is a punctured convolution code with a mother code having a constraint length k of 7 and a coding rate of 1/2. The generating polynomial of the mother code must be $G1 = 171_{oct}$ and $G2 = 133_{oct}$, shown in Fig. 2.7.

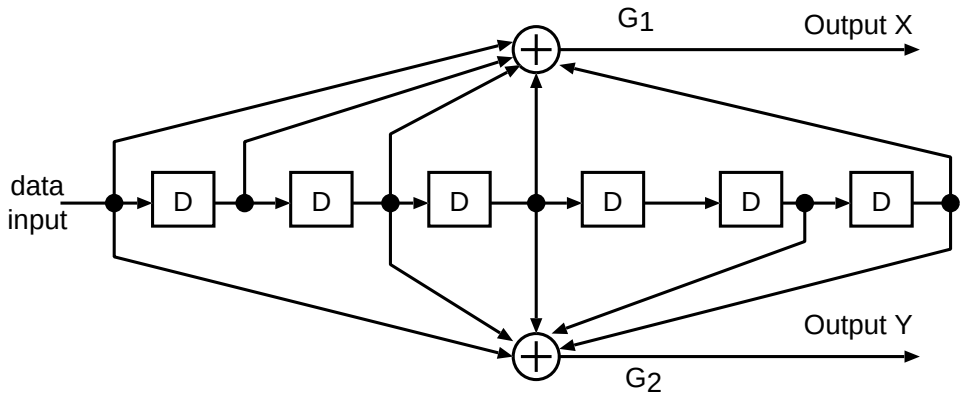

Figure 2.7. Convolution code with constraint length k of 7 and a coding rate of 1/2

ISDB-T also offers time interleaving to provide powerful channel coding for mobile-reception in which variations in field strength are inevitable. It is also shown in Fig. 2.6, that the BST-OFDM based ISDB-T has spectral multi-layer frame pattern. Up to three layers can be provided in one terrestrial channel. In the parallel processor, digital data-processing steps including error-correction

coding, interleaving and carrier modulation are primarily conducted.

It is worthy mentioning that interleaving, as an error correction technique, is adopted by many communication systems. Interleaving technique can be used nearly every procedure of signal encoding, including byte interleaving, bit interleaving, time interleaving and frequency interleaving. As we all known, time interleaving is quite effective to improve both robustness against impulsive noise and performance for portable reception. Flexible time interleave, as an error correction technique, is a special feature of ISDB-T, in contrast to the other two DTTB standards. From Fig. 2.6, the length of time interleaving is optional with a wide range from 0ms to 880ms, which makes the receivers robust against impulsive noise.

The carrier modulation type is also an optional parameter. The input signal is bit-interleaved and mapped through the schemes specified for each hierarchical layer. In terms of the transmission situation, there are 4 types of modulation processes that can be used, including DQPSK, QPSK, 16QAM and 64QAM.

Error correction, interleaving length and the carrier modulation type are specified for one hierarchical layer independently. In order to perform demodulation and decoding in hierarchical transmission in which multiple sets of transmission parameters are used, a TMCC (Transmission and Multiplexing Configuration Control) signal is also transmitted using specific carriers. The TMCC signal forms the OFDM frame together with program signals and pilot signals for synchronization and reproduction purposes.

According to the ISDB-T standard, two kinds of pilot signals are employed, scattered pilot and continual pilot. The scattered pilot is a BPSK signal that correlates output bit sequence W_i of the PRBS (Pseudo Random Bit Sequence) generating circuit shown in Fig. 2.8, where the i of W_i corresponds to the carrier number i of OFDM segment. The initial value of the PRBS-generating circuit is defined for each segment. The continual pilot is also a BPSK modulated in accordance with the carrier position (carrier number within a segment) into which it is to be inserted, and also in accordance with the W_i value. The phase angle of continual pilot determined with respect to carrier position is constant in every symbol. Once formation of a frame is complete, all signals are converted to time-domain OFDM transmission signal by IFFT.

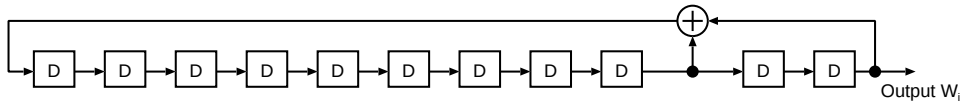

Figure 2.8. PRBS-generating polynomial and circuit for scattered pilot

6. Transmission Spectrum Arrangement of ISDB-T

In general, the carrier frequency must be the center frequency of the frequency bandwidth. And as mentioned above, ISDB-T has three transmission modes, so the OFDM sub-carrier of ISDB-T is arranged as Table. 2.3

Table 2.3. OFDM sub-carrier number corresponding to the sub-carrier frequency

Transmission mode	Mode 1	Mode 2	Mode 3
Sub-carrier number corresponding to the center frequency	702	1404	2808

And the ISDB-T program signal carrier frequency must be shifted upward by 1/7MHz (142.857kHz) from the center frequency used in the current television channel, shown in Fig. 2.9

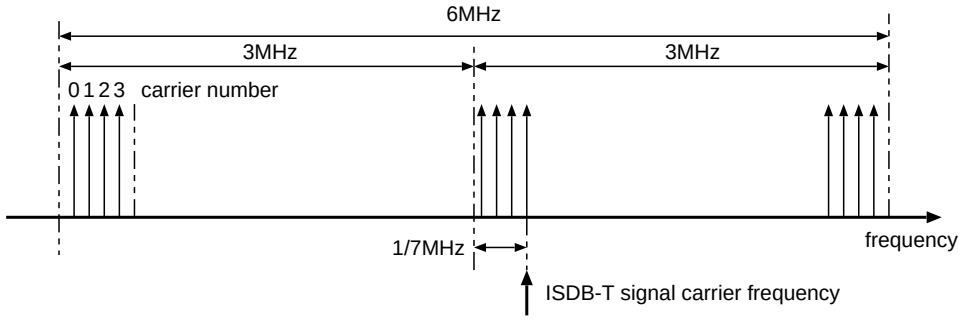

Figure 2.9. Example of ISDB-T signal frequency arrangement

Chapter 3

Impact of Impulsive Noise on ISDB-T Systems

1. Introduction

Although ISDB-T, as a multi-carrier modulation technique, is the most robust against impulsive noise among three major DTV standards for its flexible time interleaving process as mentioned in chapter 2, it is still seriously affected from the impulsive noise, since the practical energy of impulsive noise causes so strong impact to OFDM signal. This chapter mainly investigates the mathematical model and the impact of impulsive noise on ISDB-T receivers.

2. Impulsive Noise Model

Impulsive noise is a special noise that has high instantaneous power and unpredictable burst time. Usually, it is subjectively described as a kind of noise characterized by one or more short pulses whose amplitude, duration and time of occurrence are random. Many impulsive noise models have been proposed in the literature. However, it is still difficult to define impulsive noise with an absolutely precise mathematical model that can represent all the different kinds of "burst" signals in all communication systems. Some describe the impulsive noise memoryless model with a characteristic probability density function, such as the

Middleton class $A/B/C$, the Bernoulli Gaussian model and the biased Gaussian model [16][17][18][19][20][21]. Whereas others consider that the impulsive noise should be memory signal [22].

2.1 Bernoulli Gaussian Model

Bernoulli-Gaussian model is an impulsive noise that has been often used for computer simulation in the discrete time domain [16]. Assume the impulsive noise to be a Bernoulli-Gaussian process that is a product of a real Bernoulli process and a complex Gaussian process. The impulsive noise im_k can be given by,

$$im_k = b_k g_k \qquad k = 0, 1, \cdots, \tag{3.1}$$

where b_k is the Bernoulli process that is an i.i.d. (Independent and Identically-Distributed) sequence of zeros and ones with $P(b_k = 1) = p$, where p is generally a very low probability, and g_k is complex white Gaussian noise with mean zero and variance δ^2. All of the above random sequences are assumed to be independent of each other. In this model, each transmitted data symbol is hit independently by an impulse with probability p and with a random amplitude g_k. Fig. 3.1 shows the pattern of Bernoulli Gaussian noise model that looks more like bit noise.

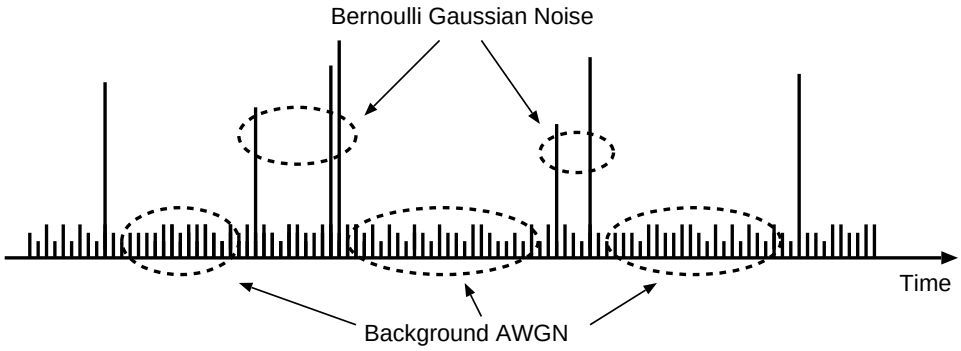

Figure 3.1. Bernoulli Gaussian noise model

2.2 Middleton's Model

Another widely adopted impulsive noise model is Middleton's model that includes three types named class A, class B and class C [17]. Class A model is a narrowband interference that arise from sources whose emission spectra are comparable to or narrower than the pass band of receivers. And Class B model is a broadband interference whose emission spectra are broader than the pass band of receivers. While the Class C is the combination of Class A and Class B. Since LPF (Low Pass Filter) and BPF (Band Pass Filter) are always set at the receivers and transmitters, the Middleton's model Class A is widely used and adopted in the literatures. Let $im(t)$ be the Class A impulsive noise whose power is normalized to be unity, $\overline{im^2(t)} = 1$. Thus for the complex channel, $im(t) = \xi(t)cos(2\pi f_c t + \phi(t))$, where f_c, $\xi(t)$ and $\phi(t)$ are denoted as a center frequency of the noise, envelope and phase, respectively. The probability density function (PDF) of the noise envelope $\xi(t)$ and the phase $\phi(t)$ are given by,

$$p_\xi(\xi) = e^{-A} \sum_{m=0}^{\infty} \frac{A^m \xi}{m! 2\pi \delta_m^2} exp(-\frac{|\xi|^2}{2\delta_m^2}) \tag{3.2}$$

$$p_\phi(\phi) = \frac{1}{\pi} \quad (0 \leq \phi < 2\pi) \tag{3.3}$$

where

$$\delta_m^2 = \delta^2 \frac{m/A + \Gamma'}{1 + \Gamma'} \tag{3.4}$$

In the above equations, Γ' is the mean power ratio of the Gaussian noise component to the non-Gaussian noise component, $\Gamma' = \delta_g^2/\delta_i^2$. And δ^2 denotes the variance of the Class A noise, while A is the impulsive index that is the product of the received average number of impulses per unit time and the duration of an impulse, $A = v_T \bar{T}_s$. The impulsive index A measures the amount of temporal overlap among the waveforms of the interfering signals. Large A, $A \to \infty$, means large overlap with a corresponding approach to Gaussian noise, while small A means highly "impulsive" interference. From the definition above, it is inferred that Middleton's model is a general noise model rather than a special model of impulsive noise. Therefore, Middleton's model is not accurate enough, in order to analyze and suppress the interference due to the impulsive noise more effectively.

2.3 Gate Gaussian Noise Model

In this chapter, we employ a new model of impulsive noise, the "Gated" Gaussian noise model, since it gives a good indication of the performance of OFDM systems for digital television broadcasting [23][24]. The gated Gaussian noise $im(t)$ is given by,

$$im(t) = n(t) \sum_{i} A_i P_{\tau_i}(t - t_i),\ i = 0, 1, \cdots, \tag{3.5}$$

where $n(t)$ is defined as normalized complex AWGN with mean zero and variance 1, and A_i is defined as a burst amplitude coefficient that is used to set the amplitude of impulsive noise. And $P_{\tau_i}(t - t_i)$ is given by,

$$P_{\tau_i}(t - t_i) = \begin{cases} 1 & |t - t_i| \leq \tau_i/2, \\ 0 & otherwise \end{cases} \quad i = 0, 1, \cdots \tag{3.6}$$

where τ_i and t_i are denoted as burst duration and arrived time of each impulsive burst, respectively. Fig. 3.2 shows a typical example of the "gated" Gaussian noise. The variance of the impulsive noise is much higher than that of AWGN, $\delta_i^2 >> \delta_w^2$, during the burst duration τ_i that is a random variable but not allowed to last more than a useful OFDM symbol. Without loss of generality, we assume that t_i follows uniform distribution in the range of OFDM symbol duration.

3. Impact of Impulsive Noise

It is assumed that the received OFDM signal suffers from two kinds of noise, additive white Gaussian noise (AWGN) and impulsive noise. The former is always regarded as background noise and discussed adequately in the literatures, while the latter can cause serious problems to the OFDM signal for its high instantaneous power and unpredictable burst time. Usually, it is subjectively described as a kind of noise characterized by one or more short pulse signal whose amplitude, duration and time of occurrence are random.

For the ISDB-T system, the information bits are mapped onto a baseband symbol S_n, and the symbol duration after serial-to-parallel (SP) conversion is T_s. Then the data sequence S_n is transformed into the time domain by IFFT; and a

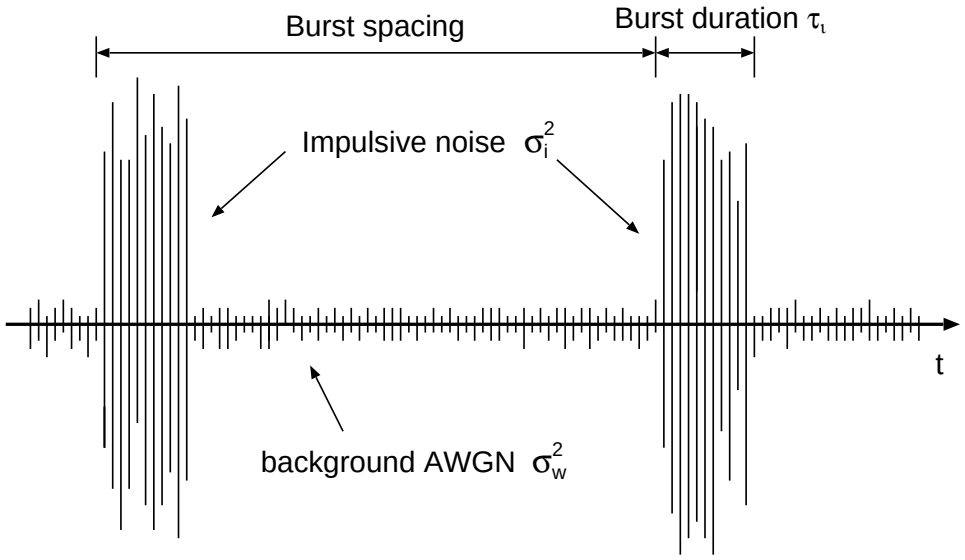

Figure 3.2. Gated Gaussian noise model

cyclic prefix (CP) that can eliminate the ISI is added at the head of the OFDM symbol as guard interval. Therefore, the transmitted OFDM signal over a block is given by,

$$s(t) = \frac{1}{\sqrt{N_F}} \sum_{n=0}^{N_F-1} S_n e^{j\frac{2\pi nt}{T_s}}, \quad -T_p \leq t < T_s \tag{3.7}$$

where N_F is the size of FFT, T_p is the length of cyclic prefix and S_n is the information symbol on the nth subcarrier. We assume that the length of channel impulse response is shorter than the CP, and the ISI can therefore be neglected in theory. Then at the ISDB-T receiver, the time-domain received signal after analog-to-digital conversion and perfect synchronization can be expressed as,

$$r_k = s_k * h_k + im_k + w_k = s'_k + im_k + w_k, k = 0, 1, \cdots, N_F - 1 \tag{3.8}$$

where $s_k = s(kT_s/N_F)$, k is defined as the time sampling index, and h_k is the channel impulse response. The operator, $*$, denotes the convolution operation, and $s'_k = s_k * h_k$. im_k and w_k are denoted as the impulsive noise and AWGN,

respectively. This procedure, attenuation from channel and noise, is also shown in Fig. 3.3. Both impulsive noise and background noise are additive noise.

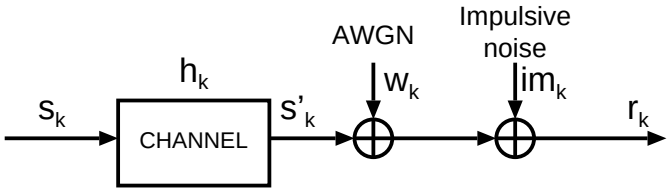

Figure 3.3. Channel and noise

In order to intuitively illustrate the interference of the impulsive noise, we classify, in Table. 3.1, the disturbance of the impulsive noise 5 classes, "weak", "medium", "slightly heavy", "heavy" and "very heavy" according to the average interference-to-signal interval ratio (ISR), which we define as $ISR = \hat{\tau}/T_s$, a ratio of the burst duration of the impulsive noise to one OFDM symbol duration with FFT size of 8192 (ISDB-T mode 3), where $\hat{\tau}$ denotes the burst duration of the impulsive noise and the active symbol duration T_s is equal to 1008μs in the case of mode 3.

Table 3.1. Disturbance class of the impulsive noise (ISDB-T mode3)

disturb class		ISR (%)	burst duration (μs)
Short Disturbance	Weak	0.5	4.9
	Medium	1	9.8
Long Disturbance	Slightly heavy	2.5	24.6
	Heavy	5	49.2
	Very heavy	10	98.4

4. Detection of Impulsive Noise

4.1 Time-domain Amplitude Threshold Detection

As an impulsive noise detection method, a time-domain detection scheme using amplitude threshold is widely used in many communication systems [16]. And the

practical applying performance demonstrates that this method is very effective to mitigate the impact from impulsive noise. However, in OFDM systems, this detection has a drawback that the determination of threshold has a great impact on the values of detected impulsive durations, and the setting of threshold becomes quite intractable. In Fig. 3.4, we notice that part of impulsive noise below the threshold would not be successfully detected.

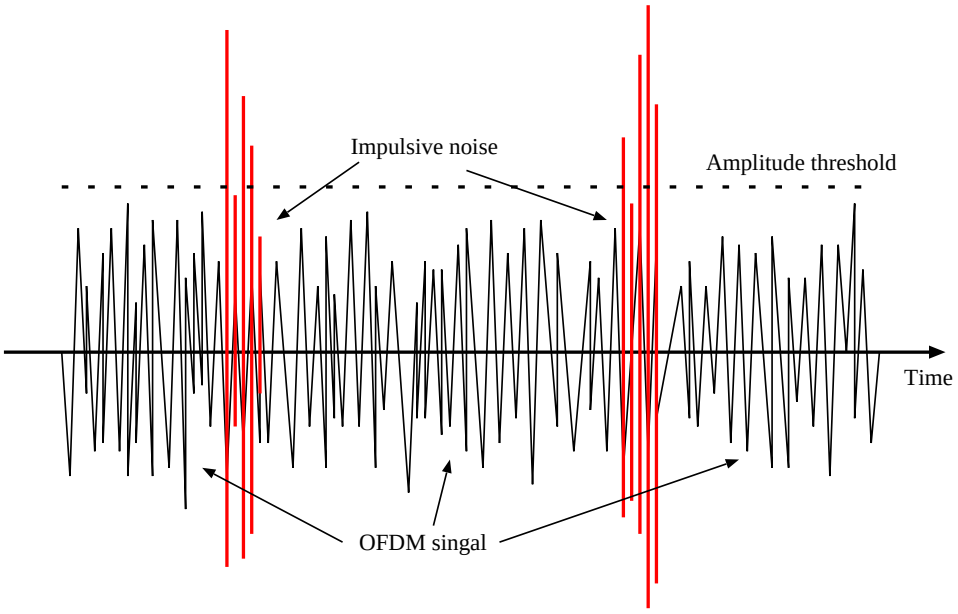

Figure 3.4. Time-domain detection by amplitude threshold

4.2 Statistial Detection by Chi-squared Test

This detection method whose block diagram is shown in Fig. 3.5, firstly needs to calculate the variance of the background noise, not including impulsive noise.

Assume the variance of background noise is σ^2. Then, a sliding observation window (SOW) is adopted to sample received signal and calculate the amplitude histogram, compare them with the chi-squared test [25], which is given by,

$$T_{chi} = \sum_{i=0}^{N-1} \frac{(X_i - x_i)^2}{x_i} \tag{3.9}$$

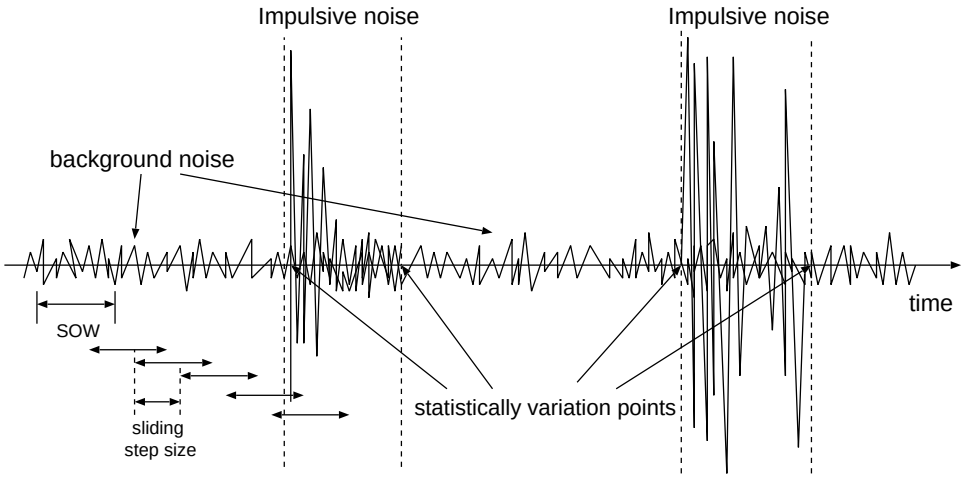

Figure 3.5. Statistial detection by chi-squared test

where N is the number of histogram bins, X_i is the value of the i-th observed bin in the range of SOW, and x_i is the value of the i-th expected bin. The i-th expected bin x_i can be calculated as

$$x_i = \int_{a_i}^{a_{i+1}} \frac{1}{\sqrt{2\pi}\sigma} \exp(-\frac{z^2}{2\sigma^2}) \mathrm{d}z, \tag{3.10}$$

If an SOW is marked as containing an impulse by the chi-square check, an additional check is performed whether significant amplitudes are present in the window. Only if this is true, the observed range will be declared to contain an impulse.

This method can be regarded as a modified time-domain threshold detection. It is very difficult to set the main parameters in this method to achieve technically precise detection similar to the conventional amplitude threshold.

Chapter 4

Joint Frequency-domain/Time-domain Method of Impulsive Noise Suppression with Adaptive Parameters for ISDB-T Receivers

1. Introduction

Since the impulsive noise is one of the most serious problems for ISDB-T receivers, in order to compensate the interference, over the last decade, a number of methods for impulsive noise suppression have been proposed in the literature. A traditional method with memoryless nonlinearity, including blanking, clipping and blanking/clipping, is simple to be implemented and practically adopted to reduce the impulsive interference by many communication systems. It usually sets an amplitude threshold to detect the peaks of received signal in time-domain and resets them to zero or a special value [26]. And the analysis, comparison and optimization of this method and its bound of BER performance is presented in [27][28]. However, the performance of the memoryless nonlinearity method is not satisfactory because the amplitude threshold of noise detection is gener-

ally decided empirically, which causes some detecting error of the impulsive noise [29]. If the impulsive noise can be detected more accurately and effectively, the performance of the nonlinearity method will be surely improved. Thus some frequency-domain noise detection schemes have been proposed by using pilot tones or special subcarriers with extreme values [30][31]. These schemes are relatively more effective than time-domain detection method, but some of the data sub-carriers are occupied, which decrease the spectral efficiency.

Recently, some indirect approaches for mitigation of impulsive interference that do not need to detect, in advance, the definite position of the impulsive noise have been developed. Häring and Vinck proposed an iterative decoding algorithm with complex number codes in which the information is exchanged between time-domain and frequency-domain [32]. And Zhidkov proposed an iteration method in which the impulsive noise would be reconstructed and subtracted from the equalized output [31]. In [33], an impulsive noise mitigation method by using decision-directed noise estimation is introduced, in which the impulsive noise component is estimated and then the opposite component of the estimated noise is reconstructed and fed back to the received OFDM signal. And this method has been developed by adding a weighted vector and extended to the case of frequency selective fading channel in [34]. In addition, a method using error-correcting code for impulsive noise cancellation is also proposed in which a posteriori control step is used to improve the decoding algorithm [35]. More recently, an iteration-based joint frequency-domain and time-domain approach is proposed that replaces the impulsive noise with the samples of the estimated signal [36]. These indirect methods improve the system performance better than the conventional nonlinearity methods, but the calculation complexity is too high for their iterative procedure.

2. Conventional Methods of Impulsive Noise Suppression

2.1 Time-domain Memoryless Nonlinear Method

The time-domain memoryless nonlinearity is widely applied at the receiver front-end before the conventional OFDM demodulator to reduce adverse effect of im-

pulsive noise [27][28]. This method depends on the statistical properties of the desired signal and non-Gaussian noise, and generally is difficult to express analytically. In practical applications, the following simple approximations are often used:

1 Blanking nonlinearity

$$y_k = \begin{cases} r_k & |r_k| \leq T_2, \\ 0 & |r_k| > T_2. \end{cases} \quad k = 0, 1, \cdots, N-1 \tag{4.1}$$

where T_2 is the blanking threshold.

2 Clipping nonlinearity

$$y_k = \begin{cases} r_k & |r_k| \leq T_1, \\ Te^{jarg(r_k)} & |r_k| > T_1. \end{cases} \quad k = 0, 1, \cdots, N-1 \tag{4.2}$$

where T_1 is the clipping threshold.

3 Clipping/Blanking nonlinearity

$$y_k = \begin{cases} r_k & |r_k| \leq T_1, \\ T_1 e^{jarg(r_k)} & T_1 < |r_k| \leq T_2, \\ 0 & |r_k| > T_2. \end{cases} \quad k = 0, 1, \cdots, N-1 \tag{4.3}$$

where T_1 is the clipping threshold and T_2 is the blanking threshold ($T_1 \leq T_2$).

The threshold of clipping and blanking has to be carefully decided to minimize the BER performance at the receivers. When threshold T_1 or T_2 is very small, most samples of the OFDM signal are clipped or reset to zeroes. Hence, some desired signal is mistakenly distorted. On the contrary, for very large value of T_1 or T_2, the memoryless nonlinear method becomes meaningless for leaving too much impulsive noise. Note that the nonlinear methods only consider the amplitude of interference (the signal's phase is not modified), therefore the nonlinearities reduce the effect of large received signal samples as these are all assumed to be the result of impulsive noise.

2.2 Decision Directed Impulsive Noise Mitigation Method

As an indirect method, decision directed estimation based impulsive noise mitigation method is also proposed [33][34][37]. Preliminary decisions are made about the transmitted data and from these an estimate is made of the noise in the received signal. The estimated noise is then subtracted from the received signal before final demodulation. When the input noise is impulsive, the method substantially reduces the noise power. The method depends on the fact that the signal appears random in the time domain and highly structured in the discrete frequency domain, whereas for the impulsive noise the converse is true. The basic block diagram of the decision directed method is described in Fig. 4.1.

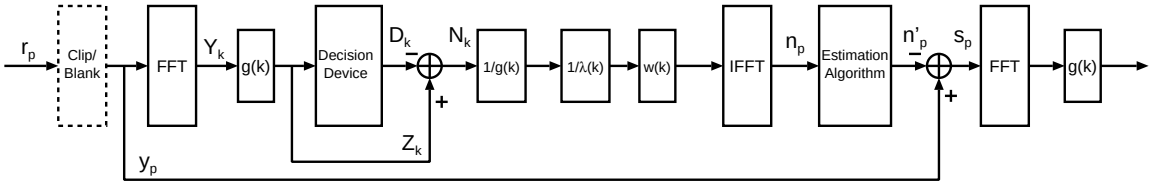

Figure 4.1. Receiver with decision directed impulsive noise mitigation

The samples r_p suffered from impulsive noise, are optionally passed through a nonlinear clipping/blanking operation. The output y_p of nonlinearity is transformed by FFT to frequency domain and we get Y_k. After equalization, the preliminary decisions, D_k about the transmitted data are made based on Z_k. From this, the "observed noise" is calculated to give $N_k = Z_k - D_k$. Except for extreme cases, most of the received subcarriers are correctly decoded and the observed noise gives accurate information about the received noise in that subcarrier. In the cases where the subcarrier is incorrectly decoded, "decision noise" will be added to the observed value. N_k is then converted back into the discrete time domain to give the time domain noise observations n_p. n_p is input to an estimation device to generate an estimate n'_p of the total input noise, which will be subtracted from y_p to generate s_p. After that, the following part is the standard procedure.

2.3 Iterative Adaptive Method for Impulsive Noise Suppression

Recently, an iterative method for impulsive noise suppression based on a priori information in frequency domain and variable threshold for impulsive noise samples detection in time domain [36]. The system block diagram of this method is shown in Fig. 4.2.

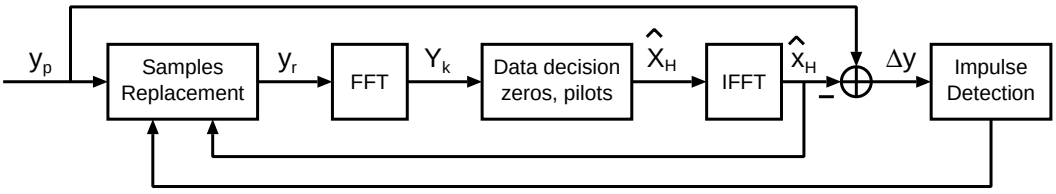

Figure 4.2. Iterative method for impulsive noise mitigation

The received signal y_p are replaced with the samples of the re-estimated signal x_H, and then the reconstructed signal y_r in time domain is obtained. The procedure can be iteratively repeated.

In first iteration, signal y_r is equal to y_p, since positions of the impulsive noise are unknown. Then, vector y_r is transformed into frequency domain to obtain signal Y_k, $Y_k = FFT(y_r)$. After that, a priori information, positions and values of pilots and inserted zeros, is used for generating signal X_H. Replace the zero subcarriers and pilots of X_H with zero and original pilot's value, respectively. X_H is then demapped for transmitted data decision $\hat{X}_H$. The frequency-domain signal $\hat{X}_H$ is transformed into time domain again by means of IFFT to get an unequalized signal $\hat{x}_H$. The iterative procedure is realized by replacing samples of the received signal y_p, which are saved in buffer in first iteration, and detected as impulsive noise. After that, the estimation of impulsive noise will be fed back to the front of the iterative procedure and enter the new iteration.

3. Proposed Scheme for Impulsive Noise Suppression

3.1 Noise Detection and Estimation in Frequency-domain

The block diagram of the proposed adaptive scheme for impulsive noise suppression is shown in Fig. 4.3. At the ISDB-T receiver, we first need to decide whether the current received OFDM symbol is affected by the impulsive noise or not. The impulsive noise decider with a fixed amplitude threshold is generally the most prevalent scheme among the conventional time-domain approaches. However this scheme is useless for the impulsive noise whose amplitude is close to the envelope of the OFDM signal in spite of being much higher than the background AWGN.

On the other hand, our proposed frequency-domain detection scheme using guard band does not occupy any useful subcarriers and can overcome the shortcoming of time-domain schemes. The active duration of the impulsive noise is very short, so its spectrum is wide enough to spread to the guard band. During the spectral band of the guard band, as shown in Fig. 4.4, there generally is no useful subcarrier of the OFDM signal, and the instantaneous energy of impulsive noise is much stronger than that of the background noise. Therefore, the impulsive noise, in the guard band, causes such a significant amplitude burst that can be observed and enable identifying the effect of the impulsive noise from the OFDM signal.

We extract the guard band signal R_{gb} from R_k that is the output of discrete Fourier transform (DFT) of the received OFDM signal, $R_k = DFT(r_k)$ where r_k is given in Eq(3.8), and calculate its instantaneous power P_{gb} in the guard band that is given by

$$P_{gb} = E\left[|R_{gb}|^2\right], \tag{4.4}$$

where $E(\cdot)$ is denoted as expectation operator. If P_{gb} exceeds the power threshold $\bar{P}_{gb}$ that is the average power of the guard band mainly generated from the background AWGN, it can be decided that this OFDM symbol is affected by the impulsive noise. After that, we need to estimate the accurate information of the impulsive noise, including noise power P_i, burst central position k_0 and active

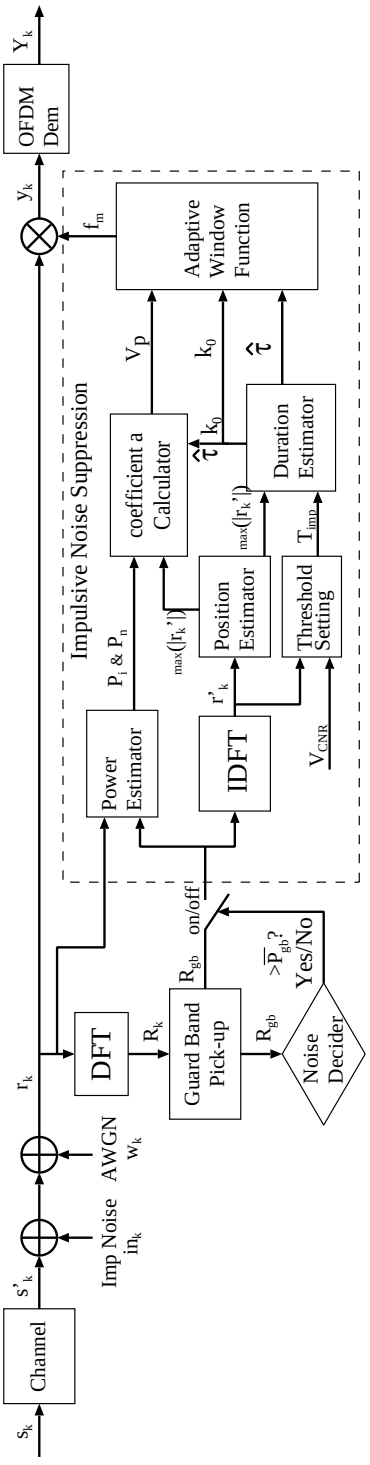

Figure 4.3. Block diagram of proposed scheme of impulsive noise suppression

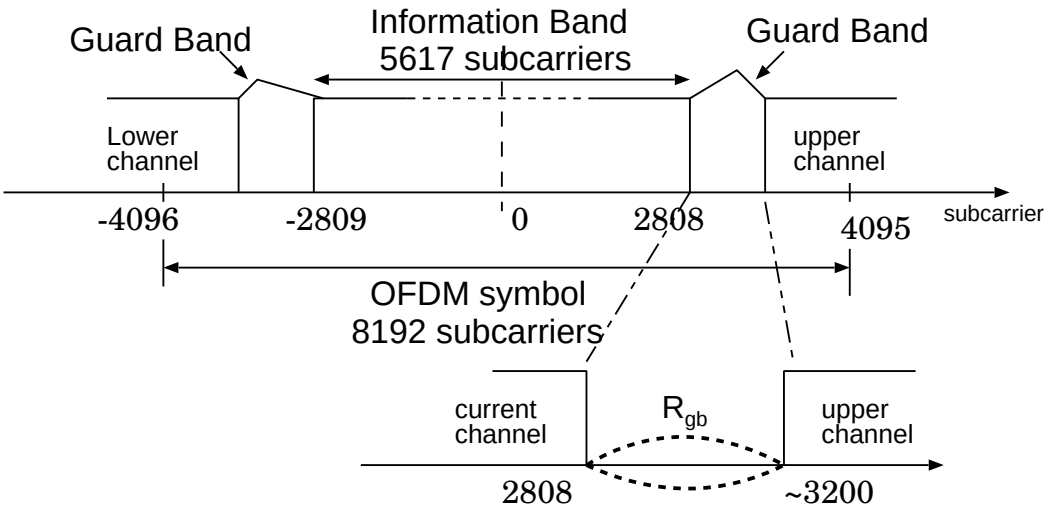

Figure 4.4. Frequency-domain detection of impulsive noise by using guard band with ISDB-T mode3

duration τ.

In order to detect the accurate burst position of the impulsive noise, R_{gb} is converted back to the discrete time domain by using Inverse Discrete Fourier Transform (IDFT) to get r'_k. The peak point of $|r'_k|$ can be decided as one burst point because of a previous decision of existence of the impulsive noise. After that, the active burst duration τ can be estimated by means of CFAR (constant false alarm rate) algorithm, which is a well-known adaptive detection algorithm used to detect target against background noise, clutter and interference in the radar receiver [38],[39]. The principle of CFAR is to determine the power threshold, and any signal that exceeds the threshold will be detected as an interference from the received signal. If the power threshold is set too low, many samples whose quantity is much more than the practical interfence will be detected at the expense of increased numbers of false alarms. Conversely, if the threshold is too high, then fewer samples will be detected, but the number of false alarms will also be low. Therefore, the threshold is usually set to achieve a required probability of false alarm.

We assume that the background noise is AWGN with slow-varying average power. And the Carrier-to-Noise Ratio (CNR) is defined as the energy ratio of

OFDM signal to background noise, CNR = P_{sig}/P_w, where P_{sig} and P_w are the power of the received OFDM signal and that of AWGN, respectively. According to general CFAR algorithms, we use an amplitude threshold T_{imp}, similar to the value of false alarm in the CFAR theorem, to separate the affected signal from the received unaffected signal. If $|r'_k| > T_{imp}$, r'_k is determined to be an affected section by the impulsive noise. The active burst duration $\hat{\tau}$ can then be estimated by counting the number of the affected points of r'_k, and we finally define the central point of $\hat{\tau}$ as the burst central position k_0.

According to the data of simulation experiments, T_{imp} can be simply defined as, $T_{imp} = \delta_w T_v$, where δ_w is the standard deviation of background AWGN and T_v is the multiplying factor. In the case of low CNR, the variance of background noise δ_w^2 is relatively large, and sometimes the amplitude of background noise even exceeds that of the OFDM signal. So we set the threshold level T_v a small value to capture the impulsive noise enough. On the other hand, in the high-CNR case, the amplitude difference between AWGN and the impulsive noise becomes distinct. Thus T_v can be set a large value to prevent capturing mistakes. In short, T_{imp} fluctuates with varying CNR. From the data of simulation experiments (see Appendix.C), T_{imp} can be calculated by,

$$T_{imp} = \delta_w \left[\left(\frac{CNR_{dB}}{10} \right)^2 + 1 \right], \tag{4.5}$$

Using this scheme, the weak impulsive noise whose burst amplitude is much higher than background noise but not high enough to be identified from OFDM signal can also be detected successfully.

In addition, there are two adjacent guard bands in one OFDM transmission channel, that is upper band and low band, as shown in Fig. 4.4. From the simulation experiment results, it is inferred that the performance of impulsive noise detection by using either two guard bands or any one of them has little difference. In order to improve the accuracy of impulsive noise detection, the guard band should be extracted totally not only a part of the guard band, since the whole guard band contains more information from interference. In addition, if the detection infers that there is no impact from impulsive noise, the next procedure of parameter estimation and impulsive noise suppression will not be

executed. It means that when the transmission channel is good enough and without impact from impulsive noise, the proposed scheme will not carry out the suppression process and save the energy cost of the ISDB-T receivers.

3.2 Noise Suppression in Time-domain

When the parameters of the impulsive noise are estimated successfully, we employ a time-domain window function to reduce the impulsive interference as a masking process. The key parameters of the window function can be adaptively adjusted in terms of the estimated information of the impulsive noise.

Conventional memoryless nonlinear methods usually adopt a rectangular window function with a fixed clipping threshold as a masking function, and for the blanking scheme, the affected OFDM signal including both the noise component and the desired signal is thoroughly blocked. Actually, the time-domain suppression schemes inevitably attenuate the desired OFDM signal and cause extra ICI along with suppression of the impulsive noise. For some obvious reasons if the pattern of the window function is just identical to the envelope of the impulsive noise, the impulsive interference can be reduced most. However it seems nearly impossible to estimate precisely and in detail the entire information about the impulsive noise without using any iteration or decision-feedback process. So we propose a sub-optimized window function with adaptive parameters to enhance the flexibility of the suppression processing. The ISDB-T receivers with impulsive noise suppression have a trade-off between noise suppression and avoiding ICI [40]. The proposed adaptive window function is given by,

$$f_m(k) = \begin{cases} 1 - \frac{V_p}{2}\left[1 + \cos\left(\frac{\pi(k-(1-\alpha)N_m)}{2\alpha N_m}\right)\right] & (1-\alpha)N_m \le (k-k_0) \le (1+\alpha)N_m \\ 1 - \frac{V_p}{2}\left[1 + \cos\left(\frac{\pi(k+(1-\alpha)N_m)}{2\alpha N_m}\right)\right] & -(1+\alpha)N_m \le (k-k_0) \le -(1-\alpha)N_m \\ 1 - V_p & -(1-\alpha)N_m < (k-k_0) < (1-\alpha)N_m \\ 1 & |(1+\alpha)N_m| < (k-k_0) \end{cases} \tag{4.6}$$

where V_p and α are denoted as the peak value and the roll-off factor of window function, respectively, and we define the adaptive width coefficient N_m by, $N_m = \hat{\tau}/2T_{samp} = \hat{\tau}N_F/2T_s$, where $\hat{\tau}$, T_{samp} are the estimated duration of impulsive noise and the sampling period, respectively. Like the conventional nonlinearity method, the adaptive window function is applied to the received signal

before OFDM demodulator, $y_k = f_m r_k$. And the main parameters of the window function can be adjusted adaptively in terms of the estimated results of the impulsive noise. The estimated duration $\hat{\tau}$ is not accurate enough to coincide with the practical width of the impulsive noise. So using the rectangular window is unavoidable to make a suppressing mistake more or less in remaining some noise components or suppressing some desired signal components. Alternatively, the pattern of the raised cosine window function is more similar to the envelope of the impulsive noise. And the raise-cosine function is transformed to frequency domain by DFT, from which the output of DFT causes less interference to other subcarriers. As mentioned in the chapter 4, we classify the disturbance of the impulsive noise 5 classes, "weak", "medium", "slightly heavy", "heavy" and "quite heavy", as shown in Table. 3.1.

For different ISR, α can be adjusted in the range $(0, 1]$ to make the pattern of the window function fit with the envelope of the impulsive noise. In fact, the ISDB-T receivers usually have some signal process blocks, including automatic gain control (AGC), band-pass filter (BPF) and low-pass filter (LPF), etc. Thus the amplitude of impulsive noise is limited to maximum threshold in the time-domain by AGC. The filters also limit the bandwidth of the impulsive noise and the edge of the impulsive noise is attenuated to decrease any sudden change. The pattern of the proposed raised-cosine window functions is similar to the output of the gated Gaussian noise passed through the filters. Note that the estimated duration of impulsive noise is not accurate enough, and its burst border is not clear either. Therefore the appropriate α is actually difficult to decide. For the short disturbance, the border duration of raised-cosine window function αN_m is also short with little interference, so choosing a large α makes the pattern of the window function more intensive to be similar to the envelope of the impulsive noise. On the other hand, for the long disturbance, the burst duration of impulsive noise becomes longer, and choosing a small α can decrease the interference to adjacent unaffected signals. Here we just adopt α, from the result of simulation experiments, with an empirical value and simply set it to 1 for short disturbances with $ISR \leq 1\%$ and 0.5 for long disturbances. The effect of the time-domain adaptive window function for impulsive noise suppression is shown in Fig. 4.5.

In addition, V_p can also be adjusted to an appropriate level of suppression in

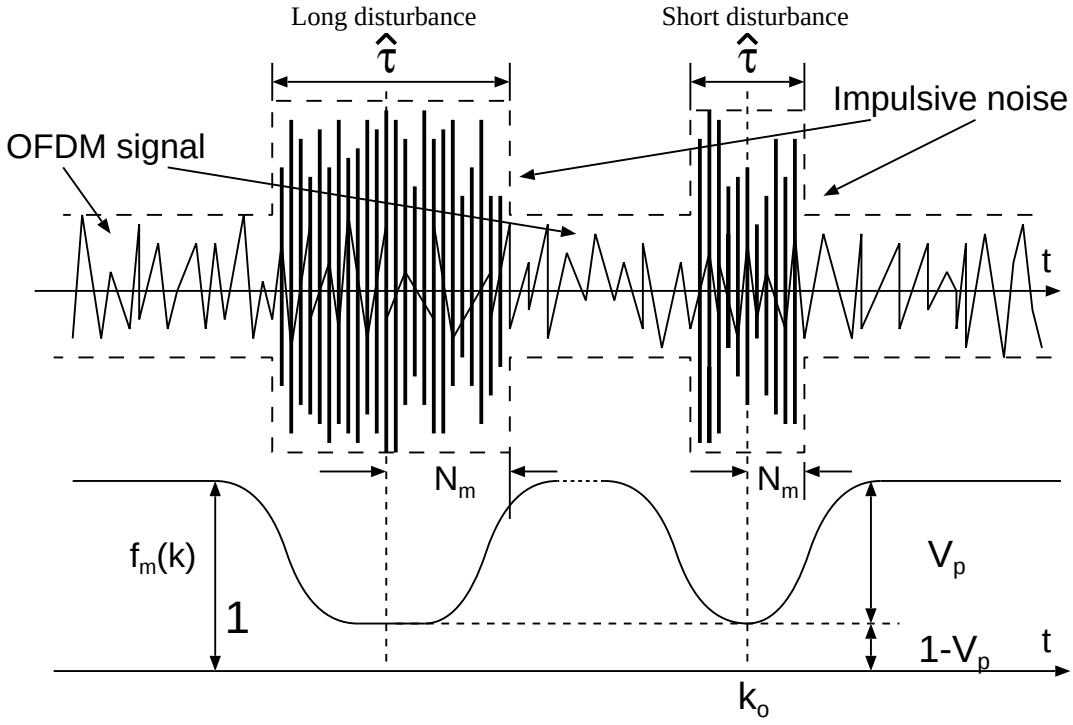

Figure 4.5. Proposed adaptive window function

order to obtain a balance between suppression and attenuation. Generally, the whole energy of OFDM signal is much more than that of the impulsive noise because of its short burst duration. So the average power of the OFDM signal P_n can be calculated in the condition of neglecting noise interference by,

$$P_n = \frac{1}{N_F} \sum_{k=0}^{N_F-1} |r_k|^2 \tag{4.7}$$

On the other hand, the amplitude of the impulsive noise is much higher than the background noise in the burst duration and the energy of the impulsive noise is spread evenly across all of the subcarriers in an OFDM symbol. For the sake of avoiding the effect of the OFDM signal, we first calculate the average power density of the impulsive noise P_i' in the frequency-domain. In the guard band, as we have known, there are only the background noise and the impulsive noise without any desired OFDM signal. The effect of the background AWGN can be neglected for its relatively weak power compared with the impulsive noise. Then, $P_i' = \frac{1}{N_{gb}} \sum_{k=0}^{N_{gb}-1} |R_{gb}(k)|^2$, where P_i' and N_{gb} denote the average power density of impulsive noise and the number of the subcarriers in the guard band, respectively. We assume that the impulsive noise is a white noise in the frequency spectrum of interest. In other words, the power density of impulsive noise follows uniform distribution in channel bandwidth. So the total energy of the impulsive noise E_z is approximately equal to the energy sum of all of the subcarriers, $E_z = N_F P_i'$. After that, we transform E_z from the frequency domain to the time domain. In the time domain, the energy of the impulsive noise focuses on the burst duration. Fortunately, the burst duration $\hat{\tau}$ of the impulsive noise has already been estimated and the type of the window function has also been decided previously. Therefore the average power P_i of the impulsive noise in the time domain can be given by,

$$P_i = \frac{E_z}{2(1+\alpha)N_m} = \frac{N_F P_i'}{2(1+\alpha)N_m} \tag{4.8}$$

$$= \frac{N_F}{2(1+\alpha)N_m N_{gb}} \sum_{k=0}^{N_{gb}-1} |R_{gb}(k)|^2 \tag{4.9}$$

After passing through the window function, part of the impulsive noise is re-

moved from the affected OFDM signal. However the time-domain nonlinear window function cannot remove the noise component entirely without attenuating any desired signal. The remained signal is the sum of the remained desired OFDM signal and the residual noise component. To facilitate analysis, we denote the removed energy of the impulsive noise E_i and the residual energy of the OFDM signal E_n that are defined as,

$$E_i = P_i \sum_{k=k_0-(1+\alpha)N_m}^{k_0+(1+\alpha)N_m} f_m^2(k) \tag{4.10}$$

$$E_n = P_n \sum_{k=k_0-(1+\alpha)N_m}^{k_0+(1+\alpha)N_m} [1 - f_m(k)]^2 \tag{4.11}$$

We certainly want to make E_i reach the maximum value for removing as much the impulsive noise as possible, while we also want to make E_n reach the maximum value simultaneously to avoid increasing extra ICI. Thus, we hope to set an appropriate peak of window function, which can make the ISDB-T receivers achieve $max(E_i + E_n)$. However, the optimum peak point is very difficult to get, since the energy of impulsive noise is not accurate enough. The function curves of E_i are in inverse proportion to that of E_n. Meanwhile, the performance's changement is relatively slow with the changement of V_p (see Fig. 4.9). So, the mask function is set to achieve a sub-optimized balance between suppression and attenuation, if we set V_p an appropriate value that makes E_i equal to E_n. After solving the equation $E_i = E_n$, V_p (see Fig. 4.5) can be calculated as,

$$V_p = \frac{2\sqrt{(\alpha^2 - 3\alpha)P_n^2 - 4(1 + 3\alpha + 2\alpha^2)P_i P_n} - 2P_n}{2((1 + 2\alpha)P_i - (1 - \frac{\alpha}{4})P_n)} \tag{4.12}$$

In brief, the proposed time-domain window function can be adjusted in terms of the adaptive parameters, including the window's depth V_p, width N_m and position k_0. Because the key parameters of the window function are adaptive, the pattern of the window function can be adjusted to fit with the envelope of the impulsive noise to obtain a sub-optimized suppression/attenuation trade-off.

4. Simulation

In order to confirm the validity of the proposed scheme, we have conducted computer simulations. In ISDB-T systems, the useful data bandwidth is about $5.57MHz$, and the assigned channel bandwidth is at least $6MHz$. In other words, a spectral bandwidth of $400kHz$ is allocated as the guard band. In addition, the ISDB-T standard includes 3 transmission modes with 2k, 4k and 8k, and in this thesis, we only discuss and analyze mode 3 (8k) whose frequency allocation has been seen in Table. 2.1; it is the most complicated and sensitive of the 3 modes. The other 2 modes can be analyzed by the same token. The main simulation parameters are summarized in Table. 4.1. In mode 3, the FFT size is 8192, and modulation type is 64QAM.

Meanwhile, we define the signal to impulsive noise ratio (SINR) by $SINR = P_{sig}/P_{in}$, where P_{sig} and P_{in} are the power of received OFDM signal and impulsive noise, respectively. As introduced before, the impulsive noise mode is the "gated" Gaussian noise of which the main parameters are all changeable, see **??**. The amplitude factor A_i is changed in terms of SINR. And the burst time t_i follows uniform distribution within the interval of an OFDM symbol. The burst duration τ_i is set according to the disturbance class and the ISR. For the medium disturbance with ISR = 1%, as an example, τ_i follows a uniform distribution with the burst duration $9.8\mu s$ and a floating range 25% more or less where the burst duration can be changed with varying ISR but the floating ratio is fixed on 25%. In order to improve the robustness of the receivers against noise further, forward error correction (FEC) and interleaving techniques have been adopted by ISDB-T receivers. We run the simulation experiment with 5000 OFDM symbols. Furthermore, in order to obtain the channel state information (CSI), we adopt a channel estimation method based on 2D Wiener filter interpolation [41].

Fig. 4.6 shows the simulation results of BER performance versus the CNR by using the proposed scheme, comparing with varying V_p (see Fig. 4.5) in the AWGN channel with medium interference. We define the CNR as the ratio of the energy of OFDM signal to the energy of AWGN, in which the effect of the impulsive noise is not considered to keep the CNR steady. And the BER performance is the statistical result from the output of the Viterbi decoder. In this figure, the system BER performance is clearly improved by using the proposed adaptive

Table 4.1. Simulation Parameters

System model	ISDB-T mode 3 (8k)
Signal bandwidth	$5.572MHz$
Channel bandwidth	$6MHz$
Guard band	$428kHz$
Impulsive noise model	Gated Gaussian noise
Disturbance classes	Short & Long (Table.3.1)
Transmission channel	AWGN & Rayleigh (TU6)
Modulation type	64-QAM
Symbol duration	1008 μs
Number of data subcarriers	5617
FFT size	8192
GI ratio	1/8
Time interleaving length	2
Convolutional code rate	3/4
Outer code	RS (204,188)

scheme with the best performance, comparing with using fixed V_p thresholds.

Fig. 4.7 shows the BER performance with the change of fixed V_p. It is clearly shown that the optimal value of T_p is relatively unstable with the change of the CNR, so the adaptive method is necessary to be adopted to achieve the optimal BER performance.

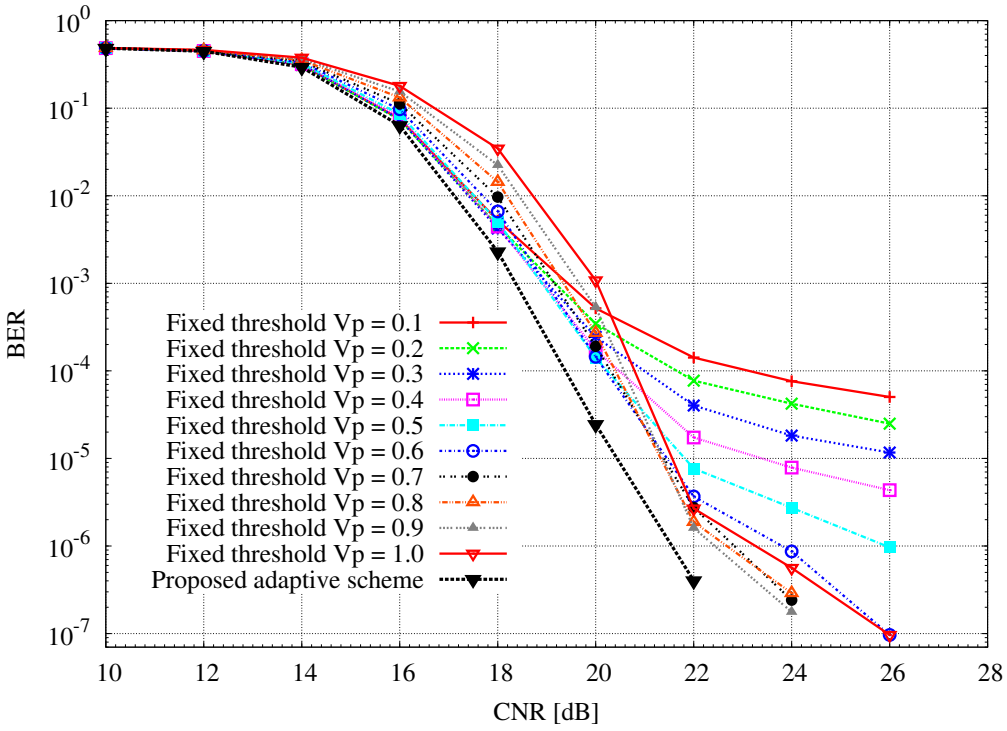

Figure 4.6. BER vs CNR, after Viterbi, SINR=-20dB, medium interference, for varying V_p threshold.

Fig. 4.8 also shows the BER performance versus the CNR, comparing with basic memoryless nonlinearity methods. From this figure, it is inferred that the proposed scheme is harmless and does not cause any other extra interference, because the curve of proposed scheme without impulsive noise coincides with the curve of ideal situation. In other words, the proposed scheme does not cause any insertion loss. And from this situation, it can be deduced that the decision of existence of the impulsive noise in frequency-domain is very accurate and effective. It is also clearly shown in this figure that the proposed scheme improves the BER

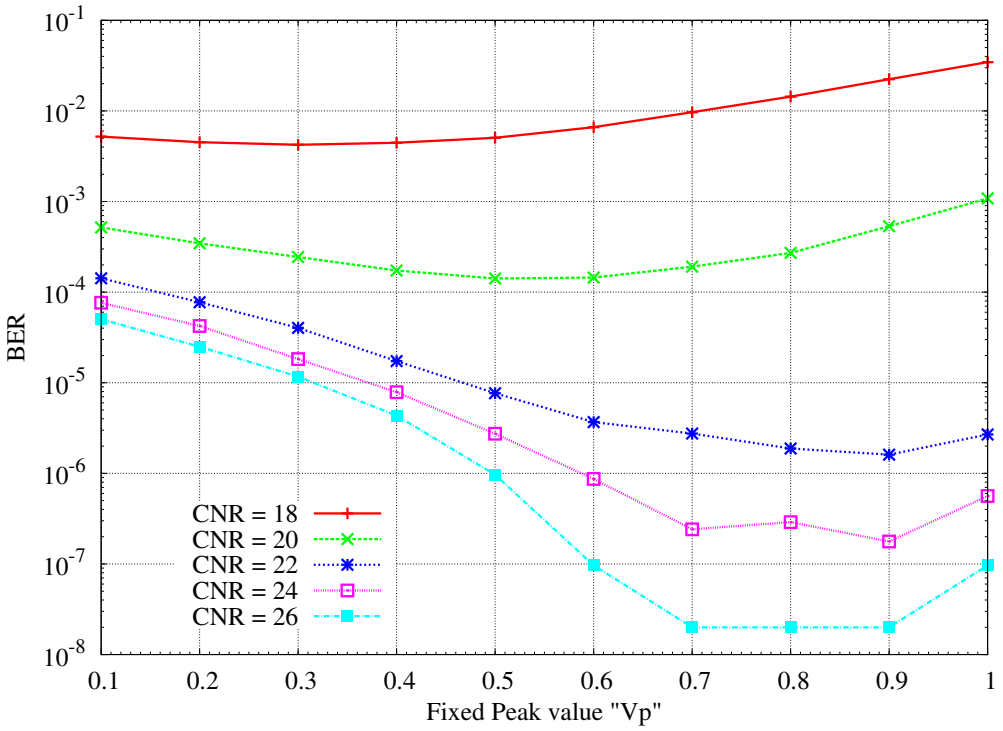

Figure 4.7. BER vs V_p, after Viterbi, SINR=-20dB, medium interference, for varying CNR.

performance to be close to the ideal performance with only 0.5dB degradation in the case of CNR = 20dB.

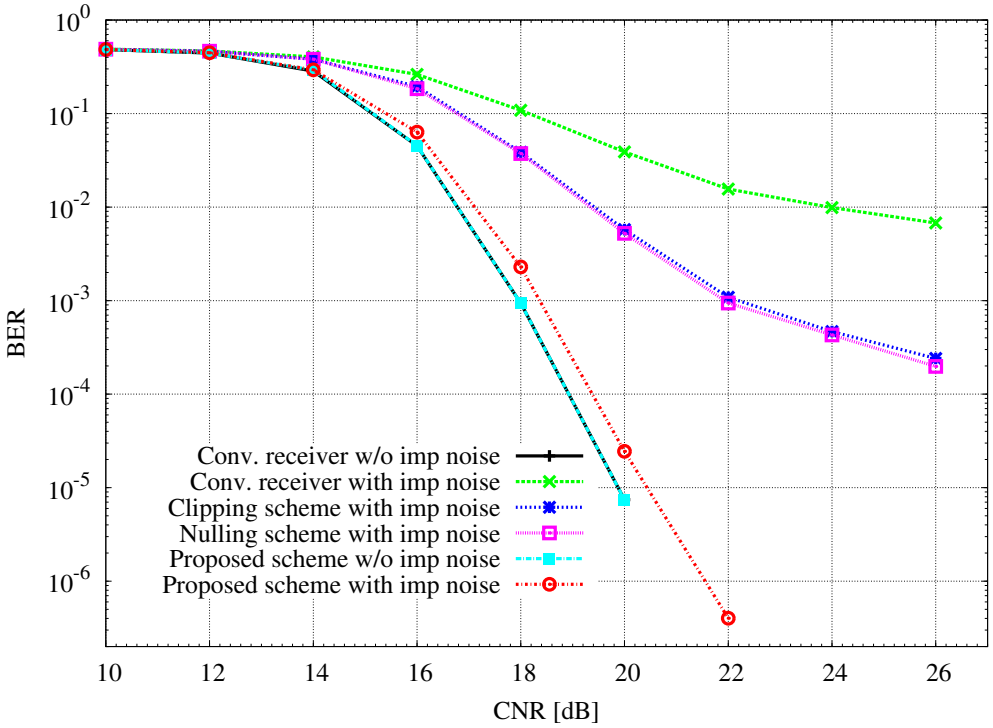

Figure 4.8. CNR vs BER, after Viterbi, SINR=-20dB, medium interference, in the AWGN channel, with different suppression schemes.

Fig. 4.9 shows the BER performance versus the CNR in Rayleigh fading channel with the dynamical multipath TU6 (Typical Urban profile made of 6 paths) and maximum Doppler shift $20Hz$. As it can be seen from this figure, the BER performance is significantly sensitive to the SINR. The BER performance is fairly degraded along with the decrease of the SINR. But for varying SINR, the proposed scheme is still effective and useful to suppress the impulsive interference and improve the system BER performance 3dB at least. And, the proposed scheme obviously works better and improves the BER performance more with heavy interference of low SINR than with weak interference of high SINR.

While in Fig. 4.10, it also shows the BER performance after RS (Reed Solomon) decoding versus the CNR with the same system parameters as in Fig. 4.9. From

this figure, we notice that the BER performance rapidly improves to very low level after RS decoding, which means that the adopted FEC process works well and effectively.

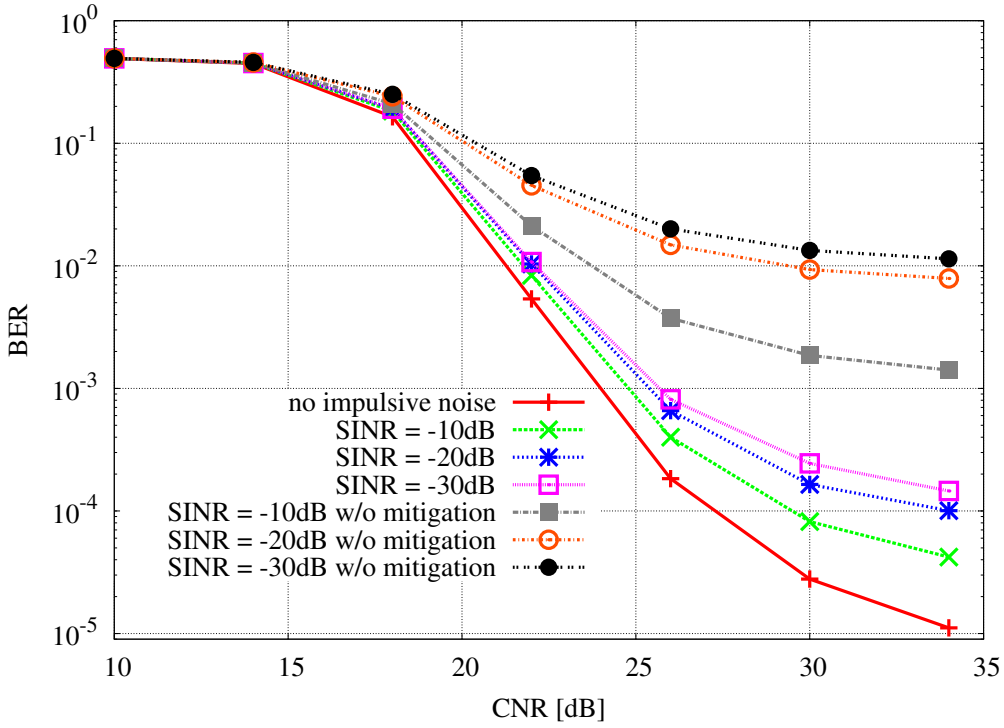

Figure 4.9. CNR vs BER, after Viterbi, medium interference, in Rayleigh fading channel, with varying SINR.

The effect of the adaptive width coefficient of the window function is shown in Fig. 4.11 with AWGN channel and Fig. 4.12 with Rayleigh fading channel, respectively. Here, we assume that every burst of impulsive noise has the identical whole energy but with varying ISR. In this case, the proposed scheme achieves a similar BER performance, in spite of varying burst duration, which implies the pattern of the window function can be effectively adjusted to fit with the envelope the impulsive noise adaptively. And it is also inferred from the figure that the burst duration of impulsive noise can be accurately estimated. Compared with the other time-domain window functions of fixed suppressing width, using the adaptive width coefficient N_m is very effective for improving the system's

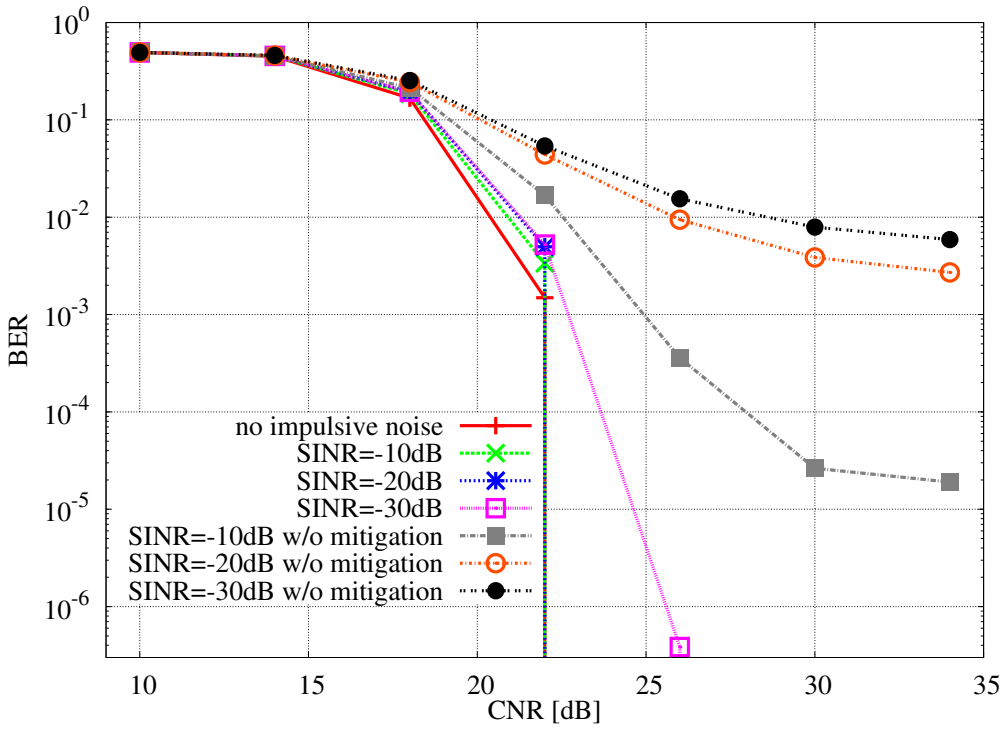

Figure 4.10. CNR vs BER, after RS decoding, medium interference, in Rayleigh fading channel, with varying SINR.

performance by enhancing the accuracy and flexibility of noise detection. In addition, with the increase of average ISR, the impulsive noise becomes flatter and flatter and is approximate to background Gaussian noise. This is similar to the degeneration in CNR, since the total energy of the impulsive noise has been assumed to be a constant and spread to all subcarriers. Therefore, the performance of the proposed scheme is slightly degraded in the case of heavy disturbance with wide burst duration.

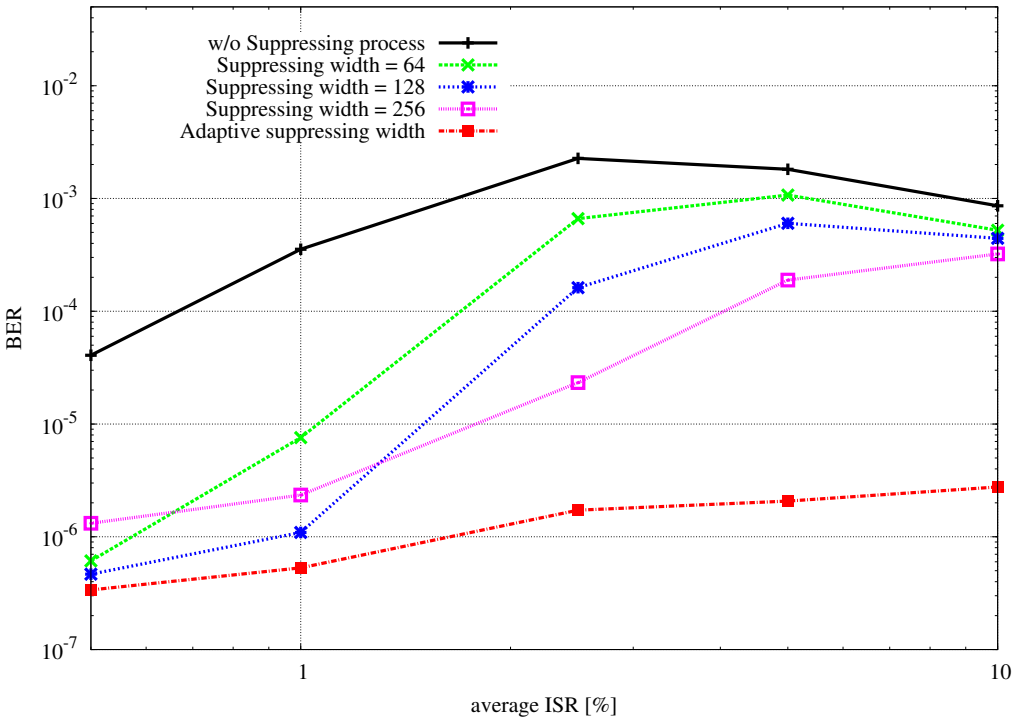

Figure 4.11. BER vs average ISR, after Viterbi, CNR=22dB in AWGN channel.

According to the ISDB-T standard, the BER performance of the receiver should not be worse than 2×10^{-4} after the Viterbi decoder, which can ensure the final BER performance after RS decoding close to zero, otherwise the OFDM signal cannot be demodulated normally and successfully. Fig. 4.13 clearly shows that the BER performance versus the SINR in the situation with CNR=20dB for AWGN channel and with CNR=34dB for Rayleigh fading channel. Since there is an automatic gain control (AGC) circuit in practical systems and analog-to-digital

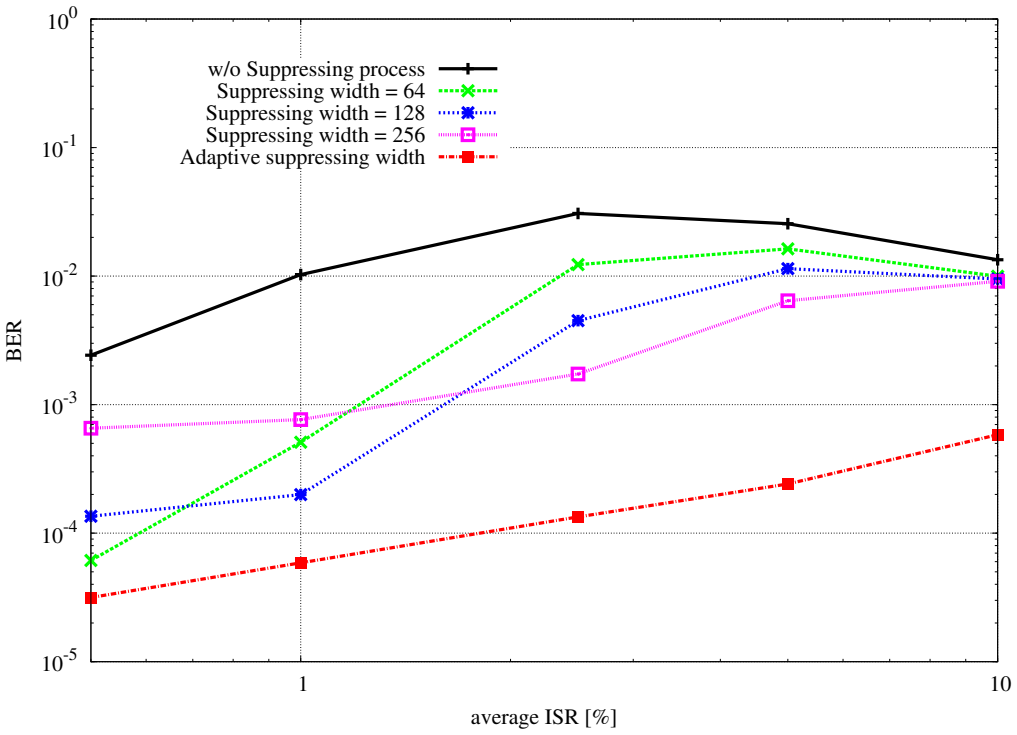

Figure 4.12. BER vs average ISR, after Viterbi, CNR=34dB in Rayleigh fading channel.

converter at the front of the receivers, the SINR seldom exceeds -30dB. Thus by using the proposed scheme, the receivers, in the condition of medium interference, can fulfill the requirement of the ISDB-T standard in both the AWGN channel and the Rayleigh fading channel.

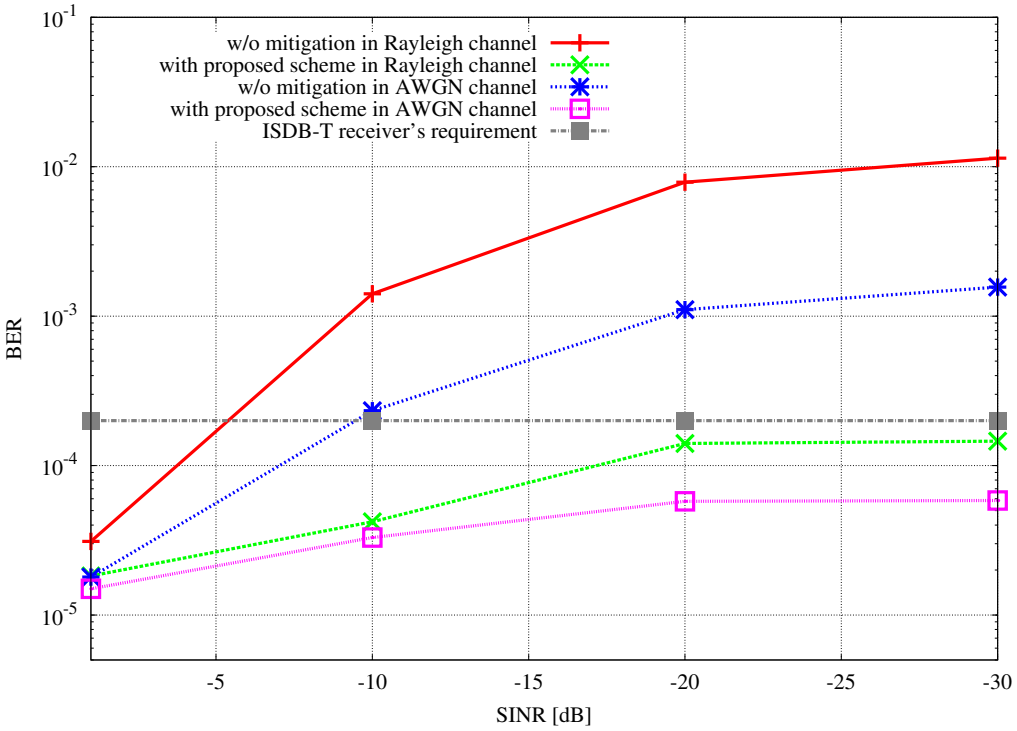

Figure 4.13. BER vs SINR, for ISDB-T standard, medium interference, CNR=20dB for AWGN channel, CNR=34dB for Rayleigh fading channel.

5. Conclusion

The impulsive noise causes serious problems for the OFDM signal at the ISDB-T receivers. We propose an adaptive scheme of impulsive noise suppression for ISDB-T receivers. Comparing with the conventional schemes, the proposed scheme combines the joint frequency-domain/time-domain noise detection and the time-domain noise suppression where the former improves the detection ac-

curacy and precision by using the guard band, and the latter achieves a suppression/attenuation trade-off by adjusting the adaptive parameters of window function. Using the proposed scheme, the major parameters of the impulsive noise can be estimated by using time-domain and frequency-domain transformation, and then an appropriate window function can also be self-adaptively constructed in terms of the estimated results.

We adopt the gated Gaussian noise as the impulsive noise model to conduct the computer simulation in the condition of ISDB-T mode 3. In the AWGN channel, by using the proposed scheme, the BER performance is degraded only 0.5dB against medium disturbance and very close to the ideal situation. Moreover the proposed scheme does not cause any insertion loss for the receivers. Similar simulation results can also be obtained in the Rayleigh fading channel. And the simulation results clearly show that the proposed scheme is effective in improving the BER performance of the ISDB-T receivers. To obtain further improvement on performance, some iterative process can be adopted after the proposed scheme.

Chapter 5

Compressed Sensing Based ICI Suppression in Fast Fading Channels

1. Introduction

Orthogonal frequency division multiplexing (OFDM) has been widely adopted in many communication fields, such as digital television broadcasting, ultra wide band (UWB), wireless LAN, etc, for its robustness and high spectral efficiency. In order to improve the system performance further, the cyclic prefix (CP) that is a copy of the tail part of the OFDM symbol is inserted into the OFDM symbols to help OFDM systems to resist the inter-symbol interference (ISI). However, the wireless transmission channels are usually multipath channels, for which the loss of the orthogonality between the subcarriers causes inter-carrier interference (ICI). Specially, for the fast fading channels, the impact of the multi-path attenuation is more significant, and the channel status information (CSI) is dynamic and even significantly changes during one OFDM symbol.

In general, the known pilot tones are previously inserted into the OFDM data subcarriers and the CSI can be estimated from the received pilot signal. The conventional pilot-assisted channel estimation methods, like Least Square (LS) and Minimum Mean-Square-Error (MMSE), have been widely adopted in the literature. The LS estimation is easy to be implemented but with poor perfor-

mance for the fast fading channels. Using some interpolation techniques, such as time-domain interpolation, low-pass interpolation and so on, can improve the performance of LS channel estimation, however the calculation complexity will be greatly increased as well. Alternatively, the MMSE estimation has high computation complexity due to the calculation of matrix inversion. As a trade-off between performance and efficiency, the Banded-MMSE estimation has been proposed later [42].

Based on the estimated results, numerous equalization methods are proposed to compensate the ICI and recover the original transmitted signal. However, conventional equalizers, such as zero-forcing equalizer [43], least-mean-square (LMS) equalizer [44], iterative equalizer [45] and so on, show some shortcomings in the fast fading channels. In order to further improve the cancellation performance, accurate estimation of channel status information (CSI) is required.

Some proposed methods actually have good performance to eliminate the ICI and keep the OFDM systems robust against fast fading channels, if the CSI can be perfectly estimated and recovered. Fortunately, the methodology of so-called "Compressed Sensing" (CS) gives us a new approach to channel estimation. As a novel methodology, CS technique has been attracted intensive attention since it was proposed several years ago [46] [47]. And it has been applied in more and more research areas, including image processing, data acquisition, radar, and so on [48] [49]. More recently, it is shown that CS technique can be used to estimate the CSI [50] [51]. And the ICI cancellation performance can be improved by efficiently using a CS-based channel estimation.

In this chapter, we propose an iterative equalization method by using CS-based channel estimation to mitigate the ICI for the time-varying fast fading channels. We use the CS-based channel estimation to recover the CSI and then eliminate the ICI by an iterative equalizer named PIC (Parallel Interference Cancellation).

2. System Model

Consider an OFDM system with N data subcarriers and the CP of length N_{cp} as guard interval. Then the transmit signal x_n, which is the output of N-point inverse discrete Fourier transform (IDFT) of source symbol sequence X_k, can be

written as

$$x_n = \frac{1}{N}\sum_{k=0}^{N-1} X_k e^{j\frac{2\pi nk}{N}}, \quad -N_{cp} \le n < N \tag{5.1}$$

Assume the channel is a time/frequency doubly-selective fading channel with time-varying impulse response $h_{n,l}$ where $l \in [0, L)$ represents the lth transmission path. The received signal y_n is then given by

$$y_n = \sum_{l=0}^{L-1} h_{n,l} x_{n-l} + w_n \tag{5.2}$$

where w_n denotes the additive white Gaussian noise (AWGN) at time n. And we assume that the CP is longer than the channel impulse response, so the inter-symbol interference (ISI) can be completely eliminated in theory by discarding the CP at the receivers. And the receiver is assumed to be perfect carrier and symbol synchronization. To recover the desired signal, y_n after CP removal is fed to frequency domain by N-point discrete Fourier transform (DFT) to obtain $Y_m = \mathrm{DFT}(y_n)$, which can be written as,

$$\begin{aligned} Y_m &= \sum_{k=0}^{N-1}\sum_{l=0}^{L-1} X_k H_l^{(m-k)} e^{-j\frac{2\pi lk}{N}} + W_m \\ &= \sum_{l=0}^{L-1} X_m H_l^0 e^{-j\frac{2\pi lk}{N}} + \\ &\quad \underbrace{\sum_{k=0,k\neq m}^{N-1}\sum_{l=0}^{L-1} X_k H_l^{(m-k)} e^{-j\frac{2\pi lk}{N}}}_{ICI} + W_m \qquad 0 \le m < N \end{aligned} \tag{5.3}$$

where W_m denotes the DFT of w_n, and $H_l^{(m-k)} = \frac{1}{N}\sum_n^{N-1} h_{n,l} e^{-j\frac{\pi n(m-k)}{N}}$ that is the DFT of $h_{n,l}$. And the first term in 5.4 is the desired part that can be easily equalized by a one-tap equalizer, while the second term represents the inter-carrier interference (ICI). For convenient denotation, 5.4 can be simplified with matrix type as

$$\mathrm{Y} = \mathrm{HX} + \mathrm{W} \tag{5.4}$$

where $\mathrm{Y} = [Y_0, \cdots, Y_{N-1}]^T$, $\mathrm{X} = [X_0, \cdots, X_{N-1}]^T$, $\mathrm{W} = [W_0, \cdots, W_{N-1}]^T$ and H is the channel matrix that needs to be estimated and reconstructed from training sequences or pilot tones. In the time-invariant channels, H is a diagonal matrix and the second term in 5.4 naturally vanishes, which means no ICI. Thus the received signal can be entirely compensated only against AWGN by a one-tap frequency-domain equalizer. However, in the case of time-varying channel, the ICI part, like an additive noise, remains after the conventional equalizers, and the residual ICI causes significant distortion, since it destroys the orthogonality between the subcarriers. And in such situation, estimating the SCI and reconstructing the channel impulse response H become the necessary procedures before OFDM demodulation. Many methods have been proposed to eliminate the ICI in literature, such as minimum mean-squared error (MMSE) equalizer, banded MMSE, self ICI cancellation schemes, iteration criterion and so on [52][53]. However all of the methods undoubtedly depend on accurate CSI estimated by different approaches. Thus it is inferred that increasing the accuracy of channel estimation can effectively improve the equalizer's performance of the OFDM systems, since the replica of ICI part can be reconstructed and subtracted from the received signal if the accurate CSI has been estimated in advance.

3. Conventional Channel Estimation Method

In order to recover the CSI, most of OFDM systems employ the scattered pilots as training sequences to realize channel estimation. The effective channel estimation methods are essential processes and have attracted researchers' concentration for a long period. Channel estimation generally is realized depending on the pilot tones based response. The known pilot subcarriers are inserted into the data subcarriers with block-type or comb-type [13], as shown in Fig. 3.

The former, block-type pilots based channel estimation, in which pilot tones are inserted into all sub-carriers of one OFDM symbol every fixed period, is developed under the assumption of slow fading channel. On the other hand, the latter, comb-type pilot based channel estimation that inserts pilot tones into certain

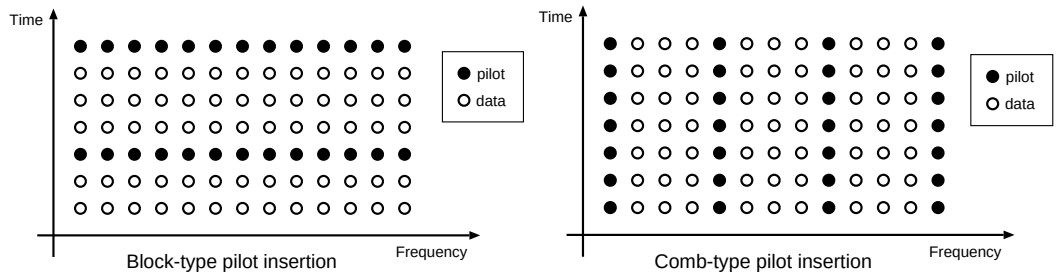

Figure 5.1. Two basic types of pilot arrangement

sub-carriers of each OFDM symbol, is introduced to satisfy the requirement for equalizing when the channel changes even within one OFDM symbol. Since there are too many approaches proposed for channel estimation, we only summarize some well-known estimators widely used as follows.

3.1 Block-type Pilot Based Channel Estimation

Matched Filter

The received vector Y can be decomposed in terms of the column vectors of H as follows:

$$\mathrm{Y} = \mathrm{h}_0\mathrm{X}_0 + \mathrm{h}_1\mathrm{X}_1 + \cdots + \mathrm{h}_{\mathrm{N}-1}\mathrm{X}_{\mathrm{N}-1} + \mathrm{W} \tag{5.5}$$

where h_k is the $(k+1)$th column vector of the matrix H. In order to detect the data $\mathrm{X_k}$, the inner product is performed between the vector Y and the vector h_k. Therefore, the decision statistic z of the matched filter is given by

$$z = \mathrm{H}^{\mathrm{H}}\mathrm{Y} = \mathrm{H}^{\mathrm{H}}\mathrm{HX} + \mathrm{H}^{\mathrm{H}}\mathrm{W} \tag{5.6}$$

where $(\cdot)^H$ denotes Hermitian transpose. Apparently, if the vector h_k are mutually orthogonal, there is no interference since the P-by-P matrix $\mathrm{H}^{\mathrm{H}}\mathrm{H}$ becomes an identity matrix. Unfortunately, this orthogonality does not hold in a fast fading channel. Hence, the matched filter suffers from ICI.

Least Square (LS)

The linear model leads to the classical least squares problem. The least squares detection statistic is given by

$$z = \mathrm{H}^{+}\mathrm{Y} \tag{5.7}$$

where the $P \times N$ matrix $\mathrm{H}^{+} = (\mathrm{H}^{\mathrm{H}}\mathrm{H})^{-1}\mathrm{H}^{\mathrm{H}}$ is the pseudo inverse of H. Without using any knowledge of the statistics of the channels, the LS estimators are calculated with very low complexity, but they suffer from a high mean-square error.

Minimum Mean Square Error (MMSE)

The MMSE detector chooses the equalizer matrix G^H which minimizes the cost function $E|d - z|^2$ where $z = G^H Y$ [54]. The resulting detection statistic becomes

$$z = G^{H}\mathrm{Y} = \mathrm{H}^{\mathrm{H}}(\mathrm{H}^{\mathrm{H}}\mathrm{H} + \delta^2\mathrm{I}_{\mathrm{N}})^{-1}\mathrm{Y} \tag{5.8}$$

where I_N is the $N \times N$ identity matrix, δ^2 is the normalized variance of the additive noise with the power of signal being supposed to be 1. As opposed to least squares, the MMSE detector requires the knowledge of the noise power. The insertion of the noise power in the inverse matrix of (5.8) reduces the noise enhancement. The MMSE has better performance than LS, especially under the low SNR (Signal-to-Noise Ratio) scenarios. A major shortcoming of the MMSE is its high computational complexity, especially if matrix inversions are needed each time the data in X changes.

3.2 Comb-type Pilot Based Channel Estimation

For time-invariance channels, there is little difference in performance between the channel estimation with block-type pilots or comb-type pilots. But in time-varying fast fading channels, the CSI changes even within one OFDM symbol, specially for some systems with long-interval frames, like digital TV broadcasting. Therefore, the schemes of channel estimation with comb-type pilots are better than with block-type pilots in time-varying channels. At the receivers, the pilots

$\mathrm{Y_p}$ are extracted from Y, then the channel conditions at the pilot subcarriers H_p^{LS} are estimated based on LS method by

$$\mathrm{H}_p^{LS} = \frac{\mathrm{Y}_p}{\mathrm{X}_p}, \quad p = 0, 1, \cdots, N_p - 1 \tag{5.9}$$

where Y_p, X_p denote the pth received and transmitted pilot, (in Fig. 3. right, the black points stand for the Y_p and X_p signal), respectively. N_p is the number of pilot subcarriers. Since N_p is less than the number of data subcarriers N, an effective interpolation technique is necessary to be adopted to estimate the channel conditions at the data subcarriers and then reconstruct the CSI.

The interpolation techniques usually used in channel estimation are linear interpolation, 2-Dimension interpolation, low-pass interpolation, spline cubic interpolation and time-domain interpolation [13]. Among them, the linear interpolation and 2D interpolation have less complexity with common performance, while the other 3 interpolation techniques have better performance but with a little high computation complexity. Generally, increasing the quantity of pilot tones can improve the accuracy of channel estimation, but it causes the decline of spectral efficiency. Recently, a so-called "compressed sensing" technique is proposed that can accurately reconstruct the original "sparse" signal with less pilot tones depending on the LS estimation. In this paper, we use the CS technique to estimate the CSI and eliminate the ICI.

Interpolation Based Estimation

In comb-type pilot based channel estimation, the response from LS estimate is limited at pilot sub-carriers. In order to estimate the full CSI including at pilot sub-carriers and data sub-carriers, an interpolation technique is necessary. A lot of interpolation methods have been proposed in the literature [12].

(A) Linear Interpolation (LI)
Linear interpolation is the simplest interpolation method that the estimation at the data sub-carriers is estimated by calculating the linear interpolation between every two pilots' response.

(B) Second Order Interpolation (SOI)
Similar to the LI, the second order interpolation estimates the CSI by

weighted linear combination of the three adjacent pilot responses.

(C) Spline Cubic Interpolation (SCI)
The spline cubic interpolation produces a smooth and continuous polynomial fitted to given data points.

(D) Low-Pass Interpolation (LPI)
The low-pass interpolation inserts zeros into the pilot response, and then the modified pilot response is transformed through a low-pass finite-length impulse response (FIR) filter. The LPI interpolates the mean-square error between the interpolated points and their ideal is minimized.

(E) Time Domain Interpolation (TDI)
The time domain interpolation firstly inserts zeros into pilot response, and then converts it to time-domain by IDFT and interpolates the time-domain sequence with some linear interpolation types. At the end, the DFT converts the interpolated time-domain sequence back to frequency domain.

The performance and calculation complexity of interpolation methods introduced above is mainly shown in Table. 5.1.

Table 5.1. Parameters of ISDB-T standard

Interpolation types	**Complexity**	**Performance**
Linear interpolation (LI)	lowest	lowest
Second order interpolation (SOI)	low	low
Spline cubic interpolation (SCI)	moderate	moderate
Time domain interpolation (TDI)	high	high
Low pass interpolation (LPI)	high	high

Least Mean Square (LMS) Estimation

The LMS estimator is an iterative estimation technique that uses a one-tap LMS adaptive filter at each pilot sub-carrier. The initial value is substituted directly

through LS and the update values are calculated based on the previous estimation [55]. The LMS method, a crude approximation of the stochastic gradient algorithm, computes $\hat{z}_n$ as

$$\hat{z}_{n+1} = \hat{z}_n + \lambda \nabla J(n) \tag{5.10}$$

where ∇ is a gradient operator, and λ is a small positive step size, $\lambda \in (0, 1)$. Generally λ is evaluated from 0 to 0.1. And $\nabla J(n) = \partial J(n)/\partial z$, where $J(n)$ is a cost function of error signal. As the step size, choosing an appropriate λ is a research. Large λ has fast convergence with low accuracy; while little λ has high accuracy with slow convergence. Computer simulations demonstrate that LMS estimation performs well, if the system is already stable. However it has the slowest convergence during the initial training sequence, which means λ is set a very little value. In time-varying channels, the LMS is sensitive and needs more time to catch the CSI change for achieving dynamic stability.

4. Equalization Methods

After channel estimation, we need to employ an equalizer for mitigating the ICI by using the reconstructed CSI. Three conventional linear equalizers are introduced as follows.

4.1 Zero-Forcing (ZF) Equalizer

The ZF equalizer is the simplest equalizer among all [43]. It contains only a one-tap equalization process that the transfer function $C(z)$ is a simple inverse filter to the channel transfer function $H(z)$, with $C = H^+$, which is shown in Fig. 5.2.

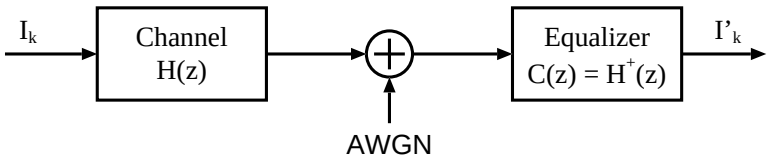

Figure 5.2. Zero-Forcing equalizer

4.2 Minimum Mean-Square-Error (MMSE) Equalizer

The ZF equalizer only cancels ISI regardless of the noise's effect. In order to minimize the combined effect of ISI and additive noise, we calculate the minimum of $E\{tr[(\hat{z}-z)(\hat{z}-z)^H]\}$, where $E\{\cdot\}$ and $tr\{\cdot\}$ denote expectation and trace of the matrix, respectively. Thus, the MMSE equalizer is denoted as

$$C = H^H(HH^H + \delta^2 I_N)^{-1} \tag{5.11}$$

where δ^2 is the normalized SNR, $\delta^2 = \delta^2_{signal}/\delta^2_{noise}$, and the matrix inversion in (5.11) requires $\mathcal{O}(N^3)$ operations.

4.3 Banded MMSE Equalizer

Though the MMSE equalizer shows better performance than ZF equalizer, the calculation complexity of inverse process in (5.11) is too high and not efficient. In [42][56], as a conclusion, the impact of ICI is focused on the central part of channel transfer matrix of frequency impulse response that is a diagonal matrix in the case of no ICI or ISI, and the rest part far from diagonal is approximate to zero. Therefore, only extracting the diagonal and some off-diagonals from the channel matrix to be the equalization matrix can greatly decrease the calculation complexity of inverse process from $\mathcal{O}(N^3)$ to $\mathcal{O}(N^2)$, and will not cause serious attenuation on the system performance. As shown in Fig. 5.3, the main diagonal entries and D off-diagonal entries are selected to construct a new band matrix.

5. Compressed Sensing

Compressed sensing (CS) is a new methodology that can realize the effective and accurate reconstruction of the original "sparse" signal from a very limited number of measurement vectors [46][57]. Consider a standard linear measurement model:

$$r = \Psi\theta + \varepsilon, \tag{5.12}$$

where r is an n-vector of responses that is the compressed signal, $\theta = (\theta_1, \theta_2, \cdots, \theta_p)^T$ is a desired "sparse" unknown p-vector in which only a few entries are non-zeros, and ε denotes a n-vector of random noise with variance σ^2. And $\Psi =$

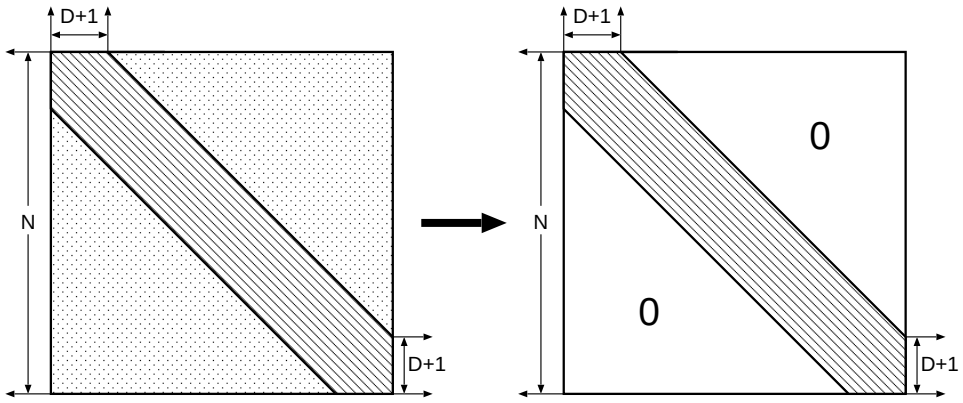

Figure 5.3. Approximation effect for windows of Banded MMSE matrix

$(\psi_1, \psi_2, \cdots, \psi_p)$ is an $n \times p$ known measurement matrix in which $\psi_i (1 \leq i \leq p)$ is measurement n-vector with $n \ll p$. For OFDM systems, Ψ can be composed of parts of the discrete Fourier transform (DFT) matrix.

As shown in Fig. 5.4, since the original signal θ is "sparse" with very limited non-zero entries, most zeros or approximate zeros can be neglected and sampled to be a compressed sequence r. After that, from the compressed sequence, the original signal can be accurately reconstructed by resolving a linear program. According to the CS technique, successfully reconstructing θ depends on two preconditions that 1) θ is sufficiently sparse and 2) the matrix Ψ that is made up of non-correlative basis, obeys a restricted condition known as the restricted isometry property [57].

5.1 Sparse Multipath Channel

Wireless channels can be categorized as either "dense" or "sparse". Dense models exhibit interarrival times of the multipath channels that are smaller than the resolvable bandwidth. While in a "sparse" channel, multipath channels arrive at time intervals that are sometimes larger than the inverse of the bandwidth of the considered channel [50]. Actually, it has been found that some practical channels, such as digital television channels [58], underwater acoustic channels [49], are sparse or approximately sparse. For example, a channel vector $h = (h_0, h_1, \cdots, h_p)$, where only n entries of p are non-zeros, is generally defined as

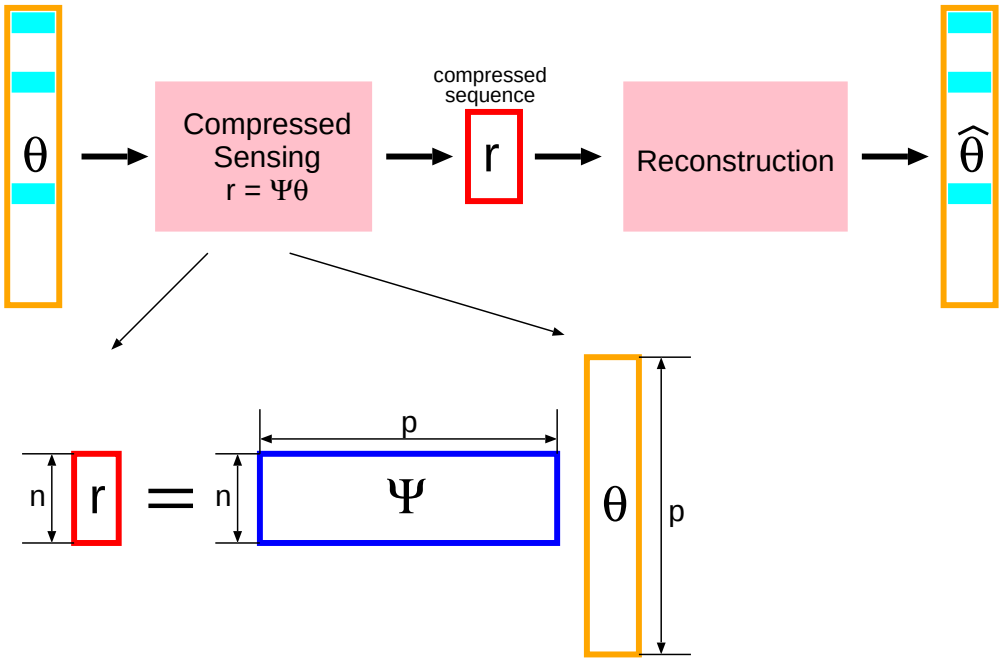

Figure 5.4. Basic model of compressed sensing

n-sparse channel.

Actually, the number of the practical transmitting paths due to scattering, reflecting, etc, is too large, practically even uncountable. So it is worth mentioning that a so-called n-sparse channel does mean that there are not really only n transmission paths, but n relatively high-energy paths with lots of very weak paths that are approximate to zero and can be neglected.

5.2 Restricted Isometry Property (RIP)

Another key condition of CS is the restricted isometry property (RIP) that has been widely accepted and extends the application range of CS [47]. Consider Ψ to be an $n \times p$ (real- and image- part) matrix that satisfies the RIP of order S with the parameter δ_S, which is written as $\Psi \in \mathrm{RIP}(S, \delta_S)$. Then define the isometry constant δ_S of Ψ as the smallest number such that

$$(1 - \delta_S)\|\theta\|_2^2 \leq \|\Psi\theta\|_2^2 \leq (1 + \delta_S)\|\theta\|_2^2 \tag{5.13}$$

holds for all s-sparse vectors, where $\|\cdot\|_2$ denotes the ℓ_2-norm. And it is defined that a vector is s-sparse if it has at most s nonzero entries.

5.3 Dantzig Selector

Since recovering the original sparse signal, according to the CS technique, depends on the solution to linear program, many methods for solving a linear program have been proposed. Two well-known methods are the Lasso and the Dantzig selector (DS) [59]. And some novel optimized methods are recently proposed, like the adaptive Lasso, DASSO, and so on [60][61]. However most of them can be regarded as the extension or improvement of the Lasso and the DS, and the difference in performance between two methods is not apparent. In fact, both of them, the Lasso and the DS, are similarly focused on the basic solution of the optimization of the linear program,

$$\theta^{CS} = \underset{\tilde{\theta} \in C^p}{\operatorname{argmin}} \|\tilde{\theta}\|_1 \tag{5.14}$$

where $\|\cdot\|_1$ denotes ℓ_1-norm and $\tilde{\theta}$ is the result of LS estimate. But they have different restricted conditions. The Lasso solution is equivalently defined as

$$\begin{aligned} \theta^{lasso} &= \underset{\tilde{\theta} \in C^p}{\operatorname{argmin}} \|\tilde{\theta}\|_1 \text{ , subject to} \\ \|(r - \Psi\tilde{\theta})\|_2^2 &= \|\Psi(\theta - \tilde{\theta})\|_2^2 \leq s \end{aligned} \tag{5.15}$$

for some non-negative s. Meanwhile the Dantzig selector (DS) can be designed as

$$\begin{aligned} \theta^{DS} &= \underset{\tilde{\theta} \in C^p}{\operatorname{argmin}} \|\tilde{\theta}\|_1 \text{ , subject to} \\ \|\Psi^H(r - \Psi\tilde{\theta})\|_\infty &= \|\Psi^H\Psi(\theta - \tilde{\theta})\|_\infty \leq \lambda \end{aligned} \tag{5.16}$$

where $\|\cdot\|_\infty$ is denoted as the ℓ_∞-norms, and $\lambda = \sqrt{2\sigma^2(1+\alpha)\log p}$ for any $\alpha \geq 0$. The norms $\|\cdot\|_1$, $\|\cdot\|_2$ and $\|\cdot\|_\infty$ are respectively defined by,

$$\|\theta\|_1 = |\theta_1| + |\theta_2| + \ldots + |\theta_n| \tag{5.17}$$

$$\|\theta\|_2 = (|\theta_1|^2 + |\theta_2|^2 + \ldots + |\theta_n|^2)^{\frac{1}{2}} \tag{5.18}$$

$$\|\theta\|_\infty = \max\{|\theta_1|, |\theta_2|, \ldots, |\theta_n|\} \tag{5.19}$$

According to the definition of CS expressed previously, the recovery of original sparse signal is equivalent to an optimization problem to solve the minimum of ℓ_1 function. Meanwhile, It is shown from (5.15) and (5.16) that the DS minimizes the ℓ_1-norm of θ subject to lying with a certain diamond, for ℓ_∞-norm, that is centered at $\tilde{\theta}$; whereas the Lasso lies within an ellipse for ℓ_2-norm with the same center [61], which is shown in Fig. 5.5.

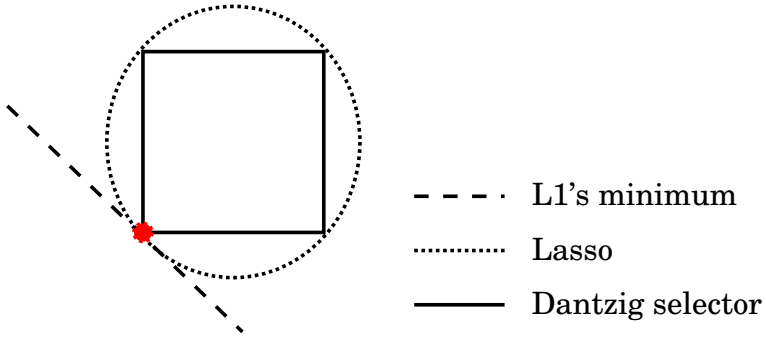

Figure 5.5. Comparison between Lasso and Dantzig selector

In [50], it is inferred that the DS is more tractable on computation than the Lasso. Therefore, we only analyze and employ the DC in the thesis. It is worthy of noticing that $\tilde{\theta}$ is a complex, so it can be decomposited into real part $\tilde{\theta}_r$ and imaginary part $\tilde{\theta}_i$, $|\tilde{\theta}| = |\tilde{\theta}_r + j\tilde{\theta}_i|$. In addition, according to the triangle inequality of absolute value, $|\tilde{\theta}|$ can be further decomposited to $|\tilde{\theta}| \approx |\tilde{\theta}_r| + j|\tilde{\theta}_i|$. Therefore, according to the description of DS, the restricted condition to linear programming is rewritten by,

$$|\Psi^H(r - \Psi\tilde{\theta})| = |\Psi^H r - \tilde{\theta}| \leq \lambda$$

$$(\Psi^H r - \lambda)_r \leq \tilde{\theta}_r \leq (\Psi^H r + \lambda)_r \tag{5.20}$$

$$(\Psi^H r - \lambda)_i \leq \tilde{\theta}_i \leq (\Psi^H r + \lambda)_i \tag{5.21}$$

Since the absolute value function $|\cdot|$ is not a linear process, we have to add an additive restricted condition that can modify $\|\tilde{\theta}\|_1$ to be satisfied with linear

process, which is written by,

$$\tilde{\theta}_r = \tilde{\theta}_r, \quad (if \quad \tilde{\theta}_r > 0) \tag{5.22}$$

$$\tilde{\theta}_i = \tilde{\theta}_i, \quad (if \quad \tilde{\theta}_i > 0) \tag{5.23}$$

$$\tilde{\theta}_r = -\tilde{\theta}_r, \quad (if \quad \tilde{\theta}_r < 0) \tag{5.24}$$

$$\tilde{\theta}_i = -\tilde{\theta}_i, \quad (if \quad \tilde{\theta}_i < 0) \tag{5.25}$$

After that, we use a linear programming software package named GLPK (GNU Linear Programming Kit) to solve $\text{argmin}_{\tilde{\theta} \in C^p} \|\tilde{\theta}\|_1$, and then recover the desired channel information.

6. Proposed Method

The system block diagram of the proposed ICI cancellation method that combines CS-based channel estimation and PIC (parallel interference cancellation) equalizer, is shown in Fig. 5.6. In the OFDM receivers, the pilot tones are extracted from the output of FFT, in which the CSI of fast fading multi-path channel is compressed and contained. Since CS-based channel estimation is developed to improve the accuracy of estimated CSI, by using it, we can reconstruct the ICI replica, which will be subtracted from the received signal within the equalization procedure. To improve the performance further, we employ an iterative equalizer of parallel interference cancellation to compensate the impact of the ICI.

6.1 CS based Channel Estimation

For simple time-delay or frequency-delay channels, the signal's distortion happens only in time-domain or frequency-domain, thus using 1-dimension DFT as measurement sequence is enough to successfully recover the CSI. However, the fast fading channels cause attenuation in both time-domain and frequency-domain. In order to estimate the accurate CSI in time/frequency doubly selective channels, 2-dimension DFT matrix is necessarily adopted to measure the CSI of the sparse channel.

Suppose that the number of the pilot subcarriers during one OFDM symbol is N_f and the number of sampled OFDM symbols for each loop is N_t. And

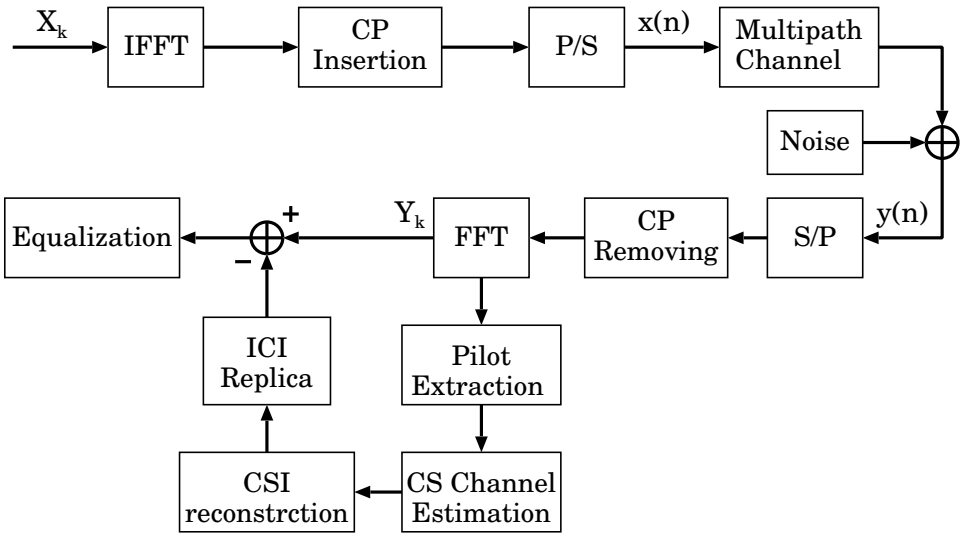

Figure 5.6. System Block diagram

K, M denote the DFT sizes in frequency-domain and time-domain, respectively. As mentioned before, we employ the DS (Dantzig Selector) to realize the CS reconstruction as a linear program. We extract the pilot tones from the received signal and calculate its frequency impulse response $H_P^{(t)}$ by

$$H_P^{(t)} = \frac{P_{Rx}^{(t)}}{P_{Tx}^{(t)}} \tag{5.26}$$

where subscript t, $(0 \leq t < M)$, is denoted as the index of sampled OFDM symbols. Meanwhile, we use the linear interpolation to obtain $H_{(t)}^{LS}$ based on $H_P^{(t)}$ in (5.26) as

$$\begin{aligned} H_{(t)}^{LS}(k) &= H_{(t)}^{LS}(mL+l), \quad 0 \leq l < L \\ &= H_p^{(t)}(m) + \frac{l}{L}(H_p^{(t)}(m+1) - H_p^{(t)}(m)) \end{aligned} \tag{5.27}$$

where $L = N/N_p$ that is the ratio of the number of the data subcarriers N to pilot tones N_p, $mL < k < (m+1)L$ and $0 \leq m < N_p$. We substitute $H_{(t)}^{LS}$ for $r_{(t)}$ in (5.16). Then, we get a KM-vector $\tilde{\theta} = [H_0^{LS}, H_1^{LS}, \cdots, H_{M-1}^{LS}]^T$, in which $H_{(t)}^{LS}$ is the K-vector of LS estimation at t-th sampled OFDM symbol. Since the

OFDM systems use DFT to modulate the orthogonal subcarriers, the measure matrix Ψ consists part of the DFT matrix. Furthermore, we use 2-dimension DFT matrix to construct the Ψ for the time/frequency doubly selective channel. Because we have to sample and process the data in both frequency axis and time axis simultaneously. Then the $N_f N_t \times KM$ measurement matrix Ψ is given below,

$$\begin{aligned} \Psi &= [1\ w_{N_f}^{n1}\ \cdots\ w_{N_f}^{n(K-1)}] \otimes \\ &\quad [w_{N_t}^{nM/2}\ w_{N_t}^{n(M/2-1)}\ \cdots\ w_{N_t}^{-nM/2}] \end{aligned} \tag{5.28}$$

where $\otimes$ is denoted as the Kronecker product, $w_N^k = e^{-j\frac{2\pi k}{N}}$ denotes an entry of DFT matrix. And the measurement matrix Ψ is full rank in column. We notice that the size of Ψ is relatively large. With the increase of K and M, the accuracy ratio of CSI recovery for time/frequency doubly-selective fading channels can be improved, as well as the computation complexity rapidly raises due to the increasing size of measurement matrix. Therefore it becomes very important to reasonably set the number of sampled OFDM symbols to take an appropriate balance between computation efficiency and recovery performance.

As an example, we suppose a 3-sparse time-delay channel with 1 direct path and 2 delay paths. It is clearly shown in Fig. 5.7 that the CS method by means of DS can accurately identify 3 paths without any noise, whereas the residual noise is very significant by using the LS estimation. Therefore, we can effectively and accurately reconstruct the CSI of transmission channel.

To confirm the proposed CS method in fast fading channels, we define a two-path doubly-selective channel with the normalized Doppler shift $[f_d T_s] = 0.25$ and 2-dimension DFT size 32×32, which means that the number of sub-carriers of one OFDM symbol is 32 and the number of sampled OFDM symbols is 32 each loop. Fig. 5.8,Fig. 5.9 and Fig. 5.10 show the orginal CSI, estimated CSI by LS method and estimated CSI by CS method, respectively. In comparison with the LS method, it is clearly shown that the reconstructed CSI by CS method is more similar to the original CSI.

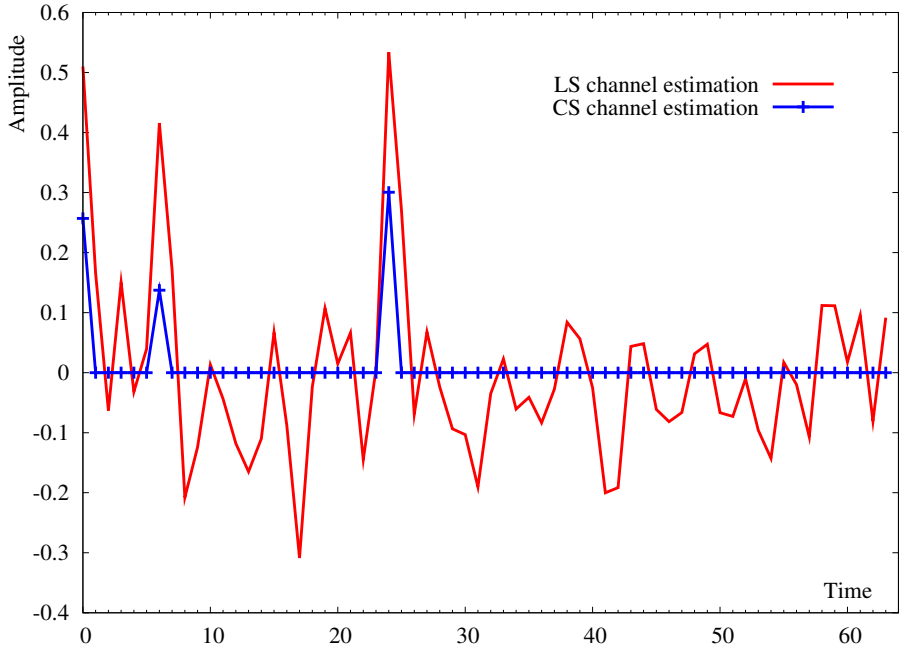

Figure 5.7. Contrasting the reconstruction abilities of LS and CS for sparse channel estimation (K=64, M=32, s=3, SNR=10dB)

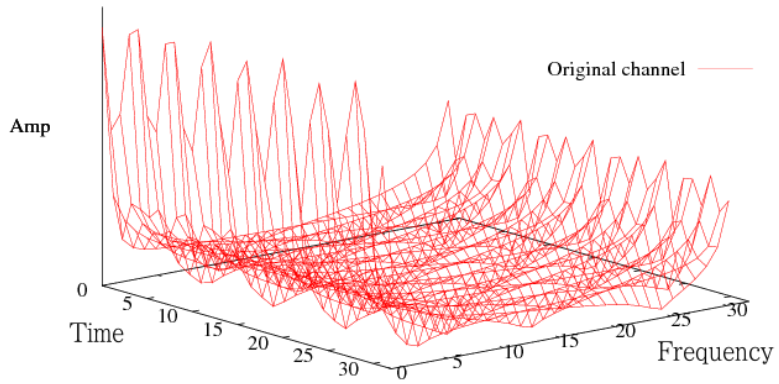

Figure 5.8. Example of original signal(K=32, M=32, s=2, SNR=20dB)

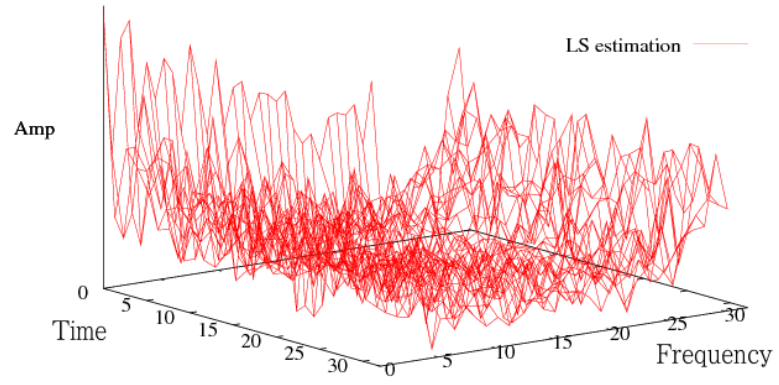

Figure 5.9. Example of LS estimated signal (K=32, M=32, s=2, SNR=20dB)

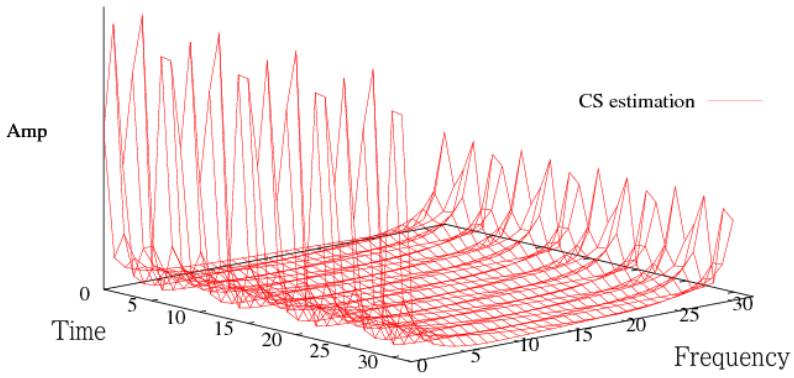

Figure 5.10. Example of CS estimated signal (K=32, M=32, s=2, SNR=20dB)

7. ICI Cancellation Based on PIC Equalizer

After CS-based channel estimation, we obtain the estimated channel impulse response and then rewrite (5.4) as

$$\mathrm{Y} = H^{cs}\mathrm{X} + \mathrm{W} \tag{5.29}$$

where H^{cs} is the estimated channel matrix based on the CS method. Suppose that $\check{H}$ is a band matrix that contains only the main diagonal and a few off-diagonals of the matrix H^{cs}. If the band matrix $\check{H}$ is used for equalization instead of H^{cs}, the calculation complexity can be effectively reduced due to the decrease on the complexity of matrix inversion. In particular, if $\check{H}$ only contains the main diagonal of H^{cs}, the inversion calculation costs only $\mathcal{O}(n)$. We adopt a low-complexity iterative equalizer of parallel interference cancellation (PIC) to mitigate the ICI [45]. First, we use the inversion of $\check{H}$ to obtain the initial equalized result.

$$X^{(0)} = \check{H}^{-1}Y \tag{5.30}$$

Then the replica of interference can be calculated by,

$$I^{(0)} = (H^{cs} - \check{H})X^{(0)} \tag{5.31}$$

After that, the reconstructed interference is subtracted from the received signal, and then we use a soft decision to calculate the $X^{(1)}$ as the beginning of the next step. Repeat the iterative process by,

$$X^{(i+1)} = \check{H}^{-1}(Y - I^{(i)}) \tag{5.32}$$

$$I^{(i)} = (H^{cs} - \check{H})X^{(i)} \tag{5.33}$$

where superscript (i) denotes the i-th iteration. If $\check{H} = diag(H^{cs})$, the complexity of inversion calculation achieves the minimum. Combine 5.32 and 5.33, we get

$$X^{(i+1)} = X^{(i)} + \check{H}^{-1}(Y - H^{cs}X^{(i)}) \tag{5.34}$$

To make $X^{(i)}$ be convergent, we need to force $X^{(i)}$ to be relocated to the nearest constellation as the soft decision. It is inferred from the simulation results that $X^{(i)}$ can quickly converge to $X^{(\infty)}$ and the iteration stops after only about three iteration steps. Since the iterative process depends on the estimated channel matrix H^{cs}, the improvement in system performance for ICI cancellation is subject to the channel estimation. To further improve the system performance, increasing the accuracy of channel estimation has probably more effective than increasing iteration steps.

8. Simulation

To confirm the potential performance of the proposed method and to compare it with conventional methods, we present some simulation results in this section. We consider an uncoded OFDM system with sub-carriers $N = 32$, a cyclic prefix with length $N_p = 8$ and QPSK modulation. The number of sampled OFDM symbols in time domain is assumed to $M = 32$. And a two-path fast fading channel is employed for the channel model. We also assume the system is perfect carrier and symbol synchronization.

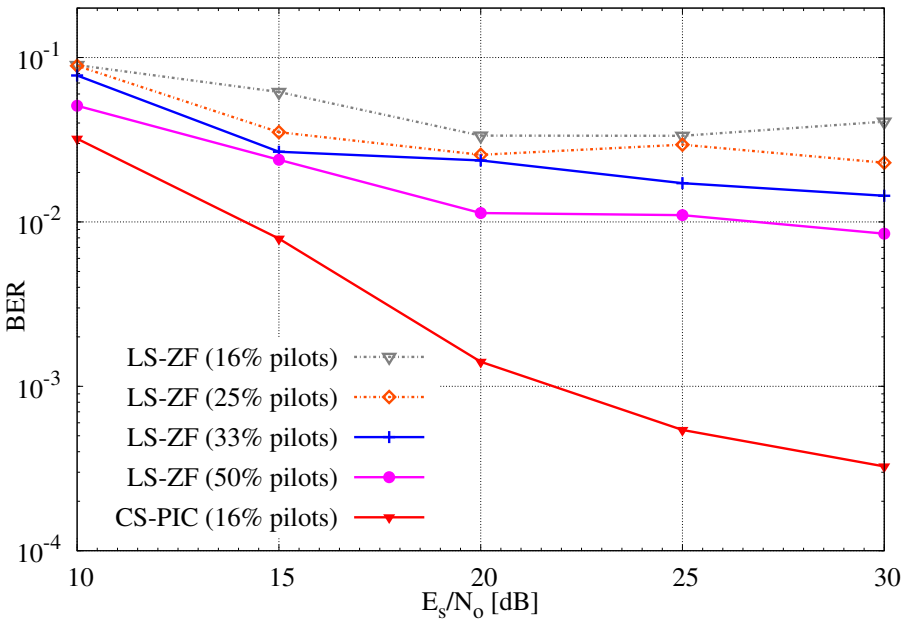

Figure 5.11. BER vs E_b/N_o, OFDM system with 32 subcarriers besides 6 pilot tones, and timedelay with 3 sampling units ($T_d = 3$)

The BER performance is shown in Fig. 5.11 against E_b/N_o. According to the CS, it can accurately recover the original data from the compressed signal with very limited pilot tones. Fig. 5.11 clearly illustrates that CS-based methods can obtain better performance even with less pilot tones and effectively improve the spectral efficiency.

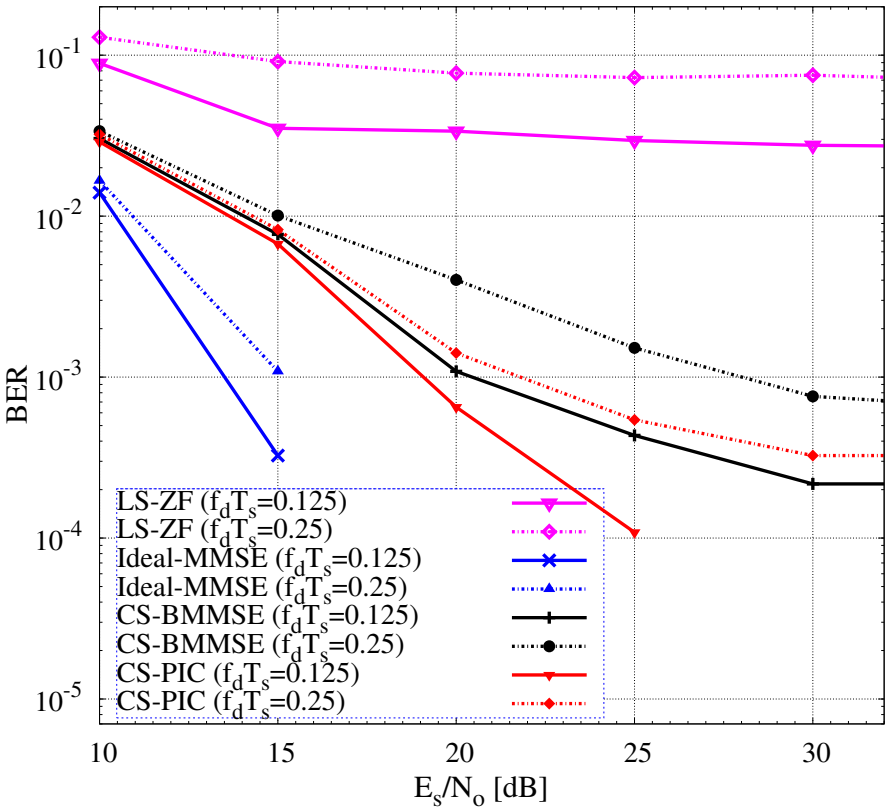

Figure 5.12. BER vs E_b/N_o, OFDM system with 32 subcarriers and 6 pilot tones and timedelay with 3 sampling units ($T_d = 3$)

Fig. 5.12 depicts the bit error rate (BER) performance against the channel signal-to-noise power ratio (SNR) with varying methods. While the conventional zero-forcing equalization that is denoted as one-tap equalizer based on LS channel estimation by means of linear interpolation has the worst performance among all the methods, the CS-based method clearly achieves much better performance

than the conventional LS methods, which implies that the recovered CSI by using CS-based method is more accurate than LS-based methods. And using the proposed PIC equalizer can further improve BER performance about 2dB, in comparison with BMMSE equalizer. The figure also shows that the same ZF equalizer based on ideal channel estimation has the best performance. It is inferred that increasing the accuracy of channel estimation can efficiently improve the system performance.

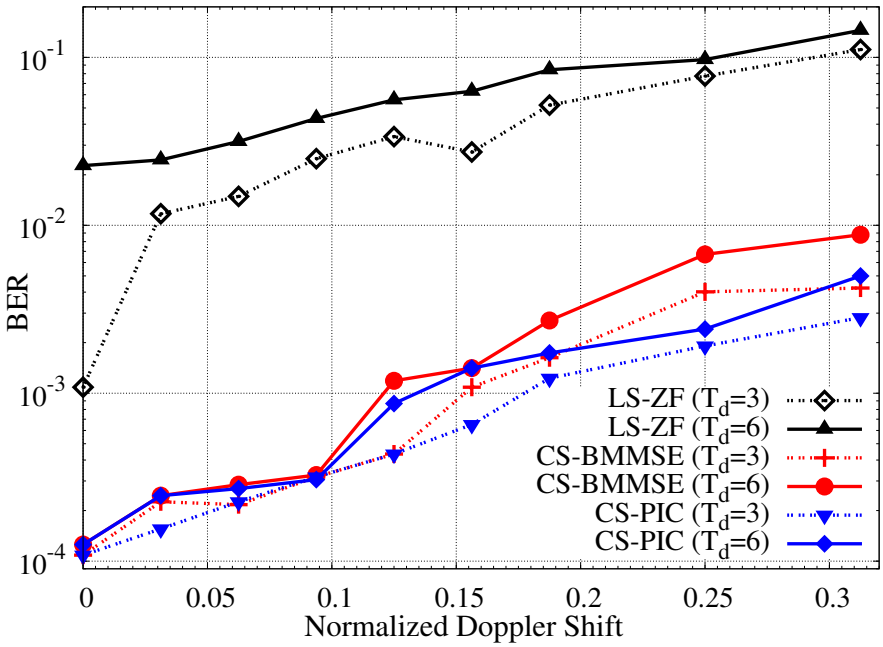

Figure 5.13. BER vs Normailized Doppler shift, OFDM system with 32 tones and E_b/N_o = 20dB in two-path fast fading channel

It is shown in Fig. 5.13 that the proposed method based on CS channel estimation is more robust to Doppler shift than the conventional LS estimation. From this figure, it is worth mentioning that the CS method is not very sensitive in the case of low normalized Doppler shift $[f_d T_s]$, where f_d and T_s are denoted as maximum Doppler shift frequency and sampling time, in which the BER performance is less different even with varying time delay and equalization methods; whereas the improvement becomes apparent with the increase on Doppler frequency shift.

We also notice that the "open" width with CS method is exactly opposite to the LS method. In low Doppler shift, LS has wide "open", whereas in contrast CS has wide "open" in the range of high Doppler shift. Comparing with LS method, the CS method is more sensitive to frequency delay than to time delay. From the estimated result of CS, it is inferred that the resolution ratio to recognize the different paths is low for low Doppler shift, because the transmission paths focus on a relatively short range of Doppler frequency shift, which makes the channel relatively "dense"; whereas the channel becomes "sparse" with the increase of the maximum Doppler shift and it is also demonstrated that the CS method shows more advantages in the sparse multipath channel.

9. Conclusion

We propose a new ICI cancellation method for OFDM systems in fast fading channels by means of CS-based channel estimation. From the computer simulation results, it is inferred that the CS technique can improve the performance of channel estimation, in particular, robust against the distortion due to noise. In contrast to the conventional channel estimation methods, CS based method does not concentrate on reconstructing the frequency-domain impulse response of transmission channel, but recovering the main coefficients of the CSI. Meanwhile, the CS-based method improves the accuracy of recovered CSI in comparison with the conventional LS-based method, the error floor of BER performance can be improved at least one order of magnitude. Moreover, the iterative PIC equalizer helps mitigating the ICI and improves BER performance further.

However, an important precondition about which we have to think is whether the channel is "sparse" enough or not. This condition restricts the application area of the CS-based channel estimation. Reducing the calculation complexity of solving linear program is also a remaining problem to which we need to be seriously faced. The proposed method is applicable to the digital television systems, including ISDB-T, DVB-T, and so on, due to its "sparse" channel character.

Chapter 6

Conclusion

The work in this thesis is focused on the improvement of system performance for ISDB-T receivers in fast fading channels. Aiming at the impulsive interference and inter-carrier interference, we propose two effective schemes to suppress the interference, respectively; the proposed methods can improve the BER performance of OFDM systems.

In order to suppress the interference of the impulsive noise, the proposed scheme focuses on more accurately detecting the existence of impact of impulsive noise in frequency-domain by means of guard band, besides the location estimation with its main parameters. If the ISDB-T system is decided not affected by impulsive noise, the process of impulsive noise suppression should not be conducted. Since the impulsive noise is a "sparse" event, improving the accuracy of decision to the impulsive noise can effectively reduce the unwanted system cost due to decrease in decision mistakes in impulsive noise. Meanwhile, the proposed scheme can be inserted into the ISDB-T receivers without adding extra interference.

On the other hand, to compensate the OFDM signal suffering from ICI, we pay main attention to the CS-based channel estimation. Since most of proposed equalization methods in the literature have an assumption of ideal channel estimation. In fact, the performance of channel estimation in fast fading channels is not good enough, so increasing the accuracy of reconstructed CSI will obtain obvious improvement on BER performance.

In Chapters 2 and 3, we overviewed the principles of OFDM technique and ISDB-T standard. In particular, the interference in fast fading channels for ISDB-

T signal is discussed in detail.

In Chapter 4, we discussed the impact of impulsive noise. The discussion started from the introduction of impulsive noise models. From many existing models, we selected a new impulsive noise model named "Gated" Gaussian noise. Of course, the impact of impulsive noise was analyzed in detail. Then the introduction to the conventional approaches to impulsive noise detection is needed.

In Chapter 5, we try to discuss a new joint frequency-domain/time-domain method of impulsive noise suppression with adaptive parameters. After the introduction to some conventional methods of impulsive noise suppression, we discuss our proposed scheme in detail. Different from the conventional amplitude threshold detection, the proposed scheme use guard band to detect impulsive noise in frequency domain. Then an adaptive window function is employed to suppress the interference from impulsive noise. From the computer simulations, the BER performance shows that the proposed scheme improves the tolerability of the ISDB-T receivers to impulsive noise.

In Chapter 6, a new CS-based ICI cancellation method has been introduced. We firstly overviewed the conventional channel estimation methods and equalization methods. And then, we introduced the CS technique in detail, including its preconditions and solutions to linear program based on CS. After that, the proposed CS-based channel estimation method was designed, and using the reconstructed CSI from the results of CS solution, we adopt a PIC equalizer to suppress the ICI in fast fading channels. The BER performance from the simulation results shows that the proposed method can effectively improve the performance of OFDM systems. And it is inferred that CS shows more significant improvement on BER performance in the case of high Doppler shift and sparser channels.

1. Future Research

The DTV has been widely adopted in Japan, not only fixed reception but also portable reception, and realization of wider spread of DTV is expected. Though most of audiences are satisfied with the broadcasting performance, there are still many serious troubles on high-speed and vehicle reception. Moreover, with the development of television and broadcasting techniques, lots of new challenges are

coming to us, such as broadcasting technique of 3D television signal, conflict between conventional TV and IPTV, and so on. So the ISDB-T standard enhancement is still going on. The future development of DTV will not be limited in pursuing technical improvement on capacity, robustness, flexibility, etc, but with more progress on multi-disciplinary techniques.

In this thesis, we study some interference suppression methods related to the effects of impulsive noise and ICI, and the computer simulations demonstrate that the proposed methods are effective to improve the system performance. However, there are still some problems needed to be solved in future. More computer simulations are going to be conducted in more complex and practical channels, including TU6, TU12, Raleigh fading channel, etc. And there is also a little improving space on the PIC equalizer. Meanwhile, optimizing the solution of linear program for CS is another important research objective. Moreover, using CS technique to detect the impulsive noise is worthy to be paid attention to.

References

References

[1] Y. Wu, E. Pliszka, B. Caron, P. Bouchard, and G. Chouinard. Comparison of terrestrial DTV transmission systems: the ATSC 8-VSB, the DVB-T COFDM, and the ISDB-T BST-OFDM. *IEEE Transactions on Broadcasting*, 46(2):101 – 113, Jun. 2000.

[2] Y. Wu, S. Hirakawa, U.H. Reimers, and J. Whitaker. Overview of digital television development worldwide. *Proceedings of the IEEE*, 94(1):8 – 21, Jan. 2006.

[3] Advanced Television Systems Committee, Inc. *A/53: ATSC digitial television standard, Parts 1-6*, Jan. 2007.

[4] ETSI EN 300 744 v1.6.1. *Digital Video Broadcasting (DVB): Framing structure, channel coding and modulation for digital terrestrial television*, Jan. 2009.

[5] Association of Radio Inductries and Businesses. *Transmission system for digital terrestrial television broadcasting (STD-B31, v1.6)*, Nov. 2005.

[6] R.A. Burger, G. Iacovoni, C. Reader, Xiaming Fu, Xiaodong Yang, and Wang Hui. A survey of digital TV standards China. In *Communications and Networking in China, 2007. CHINACOM '07. Second International Conference on*, pages 687 – 696, Aug. 2007.

[7] M. Liu, M. Crussiere, J.-F. Helard, and O.P. Pasquero. Analysis and performance comparison of DVB-T and DTMB systems for terrestrial digital

TV. In *Communication Systems, 2008. ICCS 2008. 11th IEEE Singapore International Conference on*, pages 1399 – 1404, Nov. 2008.

[8] C. Ong, J. Song, C. Pan, and Y. Li. Technology and standards of digital television terrestrial multimedia broadcasting. *Communications Magazine, IEEE*, 48(5):119 – 127, May. 2010.

[9] J. Song, Z. Yang, L. Yang, K. Gong, C. Pan, J. Wang, and Y. Wu. Technical review on Chinese digital terrestrial television broadcasting standard and measurements on some working modes. *Broadcasting, IEEE Transactions on*, 53(1):1 – 7, Mar. 2007.

[10] J. Häring and A. J. HanVinck. OFDM transmission corrupted by impulsive noise. In *Int. Symp. Powerline Communications (ISPLC), Limerick, Ireland*, pages 9 – 14, Apr. 2000.

[11] S. Kim and G.J. Pottie. Robust OFDM in fast fading channels. In *Global Telecommunications Conference, 2003. GLOBECOM '03. IEEE*, volume 2, pages 1074 – 1078, Dec. 2003.

[12] Y. Shen and E. F. Martinez. Channel estimation in OFDM systems. *AN3059, Freescale Semiconductor, Inc.*, pages 1 – 16, Jan. 2006.

[13] S. Coleri, M. Ergen, A. Puri, and A. Bahai. Channel estimation techniques based on pilot arrangement in OFDM systems. *Broadcasting, IEEE Transactions on*, 48(3):223 – 229, Sep. 2002.

[14] F.B. Frederiksen and R. Prasad. An overview of OFDM and related techniques towards development of future wireless multimedia communications. In *Radio and Wireless Conference, 2002. RAWCON 2002. IEEE*, pages 19 – 22, 2002.

[15] S. Trautmann, T. Karp, and N.J. Fliege. Frequency domain equalization of DMT/OFDM systems with insufficient guard interval. In *Communications, 2002. ICC 2002. IEEE International Conference on*, volume 3, pages 1646 – 1650, 2002.

[16] S.V. Vaseghi and P.J.W. Rayner. Detection and suppression of impulsive noise in speech communication systems. *Communications, Speech and Vision, IEE Proceedings I*, 137(1):38 – 46, Feb. 1990.

[17] D. Middleton. Statistical-physical models of electromagnetic interference. *Electromagnetic Compatibility, IEEE Transactions on*, EMC-19(3):106 – 127, Aug. 1977.

[18] A. Spaulding and D. Middleton. Optimum reception in an impulsive interference environment–Part I: Coherent detection. *Communications, IEEE Transactions on*, 25(9):910 – 923, Sep. 1977.

[19] M. Ghosh. Analysis of the effect of impulse noise on multicarrier and single carrier QAM systems. *Communications, IEEE Transactions on*, 44(2):145 – 147, Feb. 1996.

[20] D. Fertonani and G. Colavolpe. On reliable communications over channels impaired by bursty impulse noise. *Communications, IEEE Transactions on*, 57(7):2024 – 2030, Jul. 2009.

[21] H. Sedarat, B. Miller, and K. Fisher. Impulse noise protection for multicarrier communication systems. In *Acoustics, Speech, and Signal Processing, 2005. Proceedings. (ICASSP '05). IEEE International Conference on*, volume 3, pages 853 – 856, Mar. 2005.

[22] M. Zimmermann and K. Dostert. Analysis and modeling of impulsive noise in broad-band powerline communications. *Electromagnetic Compatibility, IEEE Transactions on*, 44(1):249 – 258, Feb. 2002.

[23] J. L. Fernàndez and J. Salter. Modelling impulsive interference in DVB-T: Statistical analysis, test waveforms and receiver performance. *EBU Technical Review*, 44(1):249 – 258, Jul. 2004.

[24] H. A. Suraweera, C. Chai, J. Shentu, and J. Armstrong. Analysis of impulse noise mitigation techniques for digital television systems. *8th International OFDM Workshop*, pages 172 – 176, Sep. 2003.

[25] D. Umehara, S. Hirata, S. Denno, and Y. Morihiro. Modeling of impulse noise for indoor broadband power line communications. In *International Symposium on Information Theory and its Applications, ISITA 2006, Seoul, Korea*, pages 195 – 200, Oct. - Nov. 2006.

[26] K. S. Al-Mawali, A. Z. Sadik, and Z. M. Hussain. Time-domain techniques for impulsive noise reduction in OFDM-based power line communications: a comparative study. In *International Conference on Communication, Computer and Power (ICCCP 2009), Muscat, Omen*, pages 368 – 372, Feb. 2009.

[27] S.V. Zhidkov. Performance analysis and optimization of OFDM receiver with blanking nonlinearity in impulsive noise environment. *Vehicular Technology, IEEE Transactions on*, 55(1):234 – 242, Jan. 2006.

[28] S.V. Zhidkov. Analysis and comparison of several simple impulsive noise mitigation schemes for OFDM receivers. *Communications, IEEE Transactions on*, 56(1):5 – 9, Jan. 2008.

[29] S.V. Zhidkov. Impulsive noise suppression in OFDM-based communication systems. *Consumer Electronics, IEEE Transactions on*, 49(4):944 – 948, Nov. 2003.

[30] M. Sliskovic. Signal processing algorithm for OFDM channel with impulse noise. In *Electronics, Circuits and Systems, 2000. ICECS 2000. The 7th IEEE International Conference on*, volume 1, pages 222 – 225, 2000.

[31] F. Abdelkefi, P. Duhamel, and F. Alberge. On the use of pilot tones for impulse noise cancellation in Hiperlan2. In *Signal Processing and its Applications, Sixth International, Symposium on. 2001*, volume 2, pages 591 – 594, 2001.

[32] J. Haring and A.J.H. Vinck. Iterative decoding of codes over complex numbers for impulsive noise channels. *Information Theory, IEEE Transactions on*, 49(5):1251 – 1260, May. 2003.

[33] J. Armstrong and H.A. Suraweera. Impulse noise mitigation for OFDM using decision directed noise estimation. In *Spread Spectrum Techniques*

and Applications, 2004 IEEE Eighth International Symposium on, Sydney, Australia,, pages 174 – 178, Aug. - Sep. 2004.

[34] J. Armstrong and H.A. Suraweera. Decision directed impulse noise mitigation for OFDM in frequency selective fading channels. In *Global Telecommunications Conference, 2004. GLOBECOM '04. IEEE*, volume 6, pages 3536 – 3540, Nov. - Dec. 2004.

[35] F. Abdelkefi, P. Duhamel, and F. Alberge. Impulsive noise cancellation in multicarrier transmission. *IEEE Transactions on Communications*, 53(1):94 – 106, Jan. 2005.

[36] J. Radić and N. Rožić. Adaptive impulse noise suppression in OFDM systems. *Electronics and Electrical Engineering.-Kaunas: Technological*, 97(1):3 – 8, Jan. 2010.

[37] J. Armstrong, M. Feramez, and H. A. Suraweera. Optimum Noise thresholds in decision directed impulse noise mitigation for OFDM. In *CSNDSP 2004, Newcastle, England*, pages 1 – 4, Jul 2004.

[38] F.C. Robey, D.R. Fuhrmann, E.J. Kelly, and R. Nitzberg. A CFAR adaptive matched filter detector. *Aerospace and Electronic Systems, IEEE Transactions on*, 28(1):208 – 216, Jan. 1992.

[39] S. Kraut, L.L. Scharf, and L.T. McWhorter. Adaptive subspace detectors. *Signal Processing, IEEE Transactions on*, 49(1):1 – 16, Jan. 2001.

[40] Z. Ma and M. Okada. Impulsive noise suppression for ISDB-T receivers based on adaptive window function. *Fundamentals of Electronics, Communications and Computer Science, IEICE Transactions on*, E94-A(11):2237 – 2245, Nov. 2011.

[41] P. Hoeher, S. Kaiser, and P. Robertson. Two-dimensional pilot-symbol-aided channel estimation by Wiener filtering. In *Acoustics, Speech, and Signal Processing, 1997. ICASSP-97., 1997 IEEE International Conference on*, volume 3, pages 1845 –1848, Apr. 1997.

[42] L. Rugini., P. Banelli, and G. Leus. Low-complexity banded equalizers for OFDM systems in Doppler spread channels. *EURASIP Journal on Applied Signal Processing*, 2006(1):1 – 13, Jan. 2006.

[43] J. G. Proakis and M. Salehi. *Digital Communications (Fifth edition)*. McGraw-Hill higher education, 2008.

[44] S. Coleri, M. Ergen, A. Puri, and A. Bahai. Channel estimation techniques based on pilot arrangement in OFDM systems. *Broadcasting, IEEE Transactions on*, 48(3):223 – 229, Sep. 2002.

[45] A.F. Molisch, M.. Toeltsch, and S.. Vermani. Iterative methods for cancellation of intercarrier interference in OFDM systems. *Vehicular Technology, IEEE Transactions on*, 56(4):2158 – 2167, Jul. 2007.

[46] D.L. Donoho. Compressed sensing. *Information Theory, IEEE Transactions on*, 52(4):1289 – 1306, Apr. 2006.

[47] E.J. Candes, J. Romberg, and T. Tao. Robust uncertainty principles: exact signal reconstruction from highly incomplete frequency information. *Information Theory, IEEE Transactions on*, 52(2):489 – 509, Feb. 2006.

[48] C.R. Berger, Zhaohui Wang, Jianzhong Huang, and Shengli Zhou. Application of compressive sensing to sparse channel estimation. *Communications Magazine, IEEE*, 48(11):164 – 174, Nov. 2010.

[49] C.R. Berger, Shengli Zhou, J.C. Preisig, and P. Willett. Sparse channel estimation for multicarrier underwater acoustic communication: From subspace methods to compressed sensing. In *OCEANS 2009 - EUROPE*, pages 1 – 8, May. 2009.

[50] W.U. Bajwa, J. Haupt, A.M. Sayeed, and R. Nowak. Compressed cannel sensing: A new approach to estimating sparse multipath channels. *Proceedings of the IEEE*, 98(6):1058 – 1076, Jun. 2010.

[51] G. Taubock and F. Hlawatsch. A compressed sensing technique for OFDM channel estimation in mobile environments: Exploiting channel sparsity for

reducing pilots. In *Acoustics, Speech and Signal Processing, 2008. ICASSP 2008. IEEE International Conference on*, pages 2885 – 2888, Apr. 2008.

[52] J. Armstrong. Analysis of new and existing methods of reducing intercarrier interference due to carrier frequency offset in OFDM. *Communications, IEEE Transactions on*, 47(3):365 – 369, Mar. 1999.

[53] Y. Ida, C. J. Ahn, T. Kamio, H. Fujisaka, and K. Haeiwa. ISI and ICI compensation for TFI-OFDM in time-variant large delay spread channel. In *23rd International Technical Conf. on Circuits/Systems, Computers and Communications (ITC-CSCC2008)*, pages 1309 – 1312, Jul. 2008.

[54] O. Edfors, M. Sandell, J.-J. van de Beek, S.K. Wilson, and P.O. Borjesson. OFDM channel estimation by singular value decomposition. *Communications, IEEE Transactions on*, 46(7):931 – 939, Jul. 1998.

[55] R. Otnes and M. Tuchler. Iterative channel estimation for Turbo equalization of time-varying frequency-selective channels. *Wireless Communications, IEEE Transactions on*, 3(6):1918 – 1923, Nov. 2004.

[56] W. G. Jeon, K. H. Chang, and Y. S. Cho. An equalization technique for orthogonal frequency-division multiplexing systems in time-variant multipath channels. *Communications, IEEE Transactions on*, 47(1):27 – 32, Jan. 1999.

[57] E. J. Candés. The restricted isometry property and its implications for compressed sensing. *Comptes Rendus Mathematique*, 346(5):589 – 592, May. 2008.

[58] Advanced Television Systems Committee, Inc. *Receiver performance guidelines, ATSC recommended practices for digital television*, Sep. 2009.

[59] E. J. Candés and T. Tao. The Dantzig selector: Statistical estimation when p is much larger than n. *Ann. Statist*, 35(6):2313 – 2351, Dec. 2007.

[60] H. Zou. The adaptive Lasso and its Oracle properties. *Journal of the American Statistical Association*, 101(476):1418 – 1429, Dec. 2006.

[61] G. M. James, P. Radchenko, and J. Lv. DASSO: connections between the Dantzig selector and Lasso. *Journal of the Royal Statistical Society*, 71(1):127 – 142, Jan. 2009.

Acknowledgements

First of all, I would like to thank my supervisor, Professor Minoru Okada, for his outstanding guidance, support and advice at all stages of this work.

Also thanks to Associate Professor Takao Hara and Assistant Professor Ryusuke Miyamoto for their continued interest, comments and suggestions. And I also would like to express my sincere gratitude to Professor Hiroyuki Seki and Professor Kenji Sugimoto for their constructive comments and positive support.

I am thankful to all the members at the laboratory of Network Systems for the enjoyable atmosphere and for their help, with particular mention to: Ibin Xin, Yanyan Ma, Satoshi Tsukamoto, Hiromi Takahata, Igeda Puja, Tomonori Sato, Shinichi Watanabe, Takehiro Ishikuro, Hiroki Kameyama, Miki Kioi, etc. Thanks also to the guys already graduated from the laboratory and to the hospitable NAIST's office clerks for their unselfish helps.

I gratefully acknowledge the financial support of the Ministry of Education, Culture, Sports, Science & Technology in Japan (MEXT) and China Scholarship Council. Thank them for giving me the necessary scholarship to complete my works.

I would like to express my deepest gratitude to my family, my dear mother and lovely wife, for their dedication, love, encouragement and support in all my endeavors.

Appendix

A. Acronyms and Abbreviation

Abbreviation	**Full Name**
AGC	Automatic Gain Control
ATSC	Advanced Television Systems Committee
AWGN	Additive White Gaussian Noise
A/D	Analog to Digital (converter)
BER	Bit Error Rate
BMMSE	Banded MMSE
BST-OFDM	Band Segmented Transmission OFDM
CFAR	Constant False Alarm Rate
CMMB	China Mobile Multimedia Broadcasting
CNR	Carrer-to-Noise Ratio
CP	Cyclic Prefix
CS	Compressed Sensing
CSI	Channel State Information
DFT	Discrete Fourier Transform
DQPSK	Differential QPSK
DS	Dantzig Selector
DSL	Digital Subscriber Line
DTMB	Digital Terrestrial Multimedia Broadcasting
DVB-T	Digital Video Broadcasting for Terrestrial
D/A	Digital to Analog (converter)
FFT	Fast Fourier Transform

FIR	Finite-length Impulse Response
GI	Guard Interval
GLPK	GNU Linear Programming Kit
HDTV	High Definition TeleVision
ICI	Inter-Carrier Interference
IDFT	Inverse Discrete Fourier Transform
IFFT	Inverse Fast Fourier Transform
ISDB-T	Integrated Services Digital Broadcasting for Terrestrial
ISI	Inter-Symbol Interference
ISR	Interference-to-Signal Ratio
LMS	Least Mean Square
LPF	Low Pass Filter
LS	Least Square
MMSE	Minimum Mean Square Error
MPEG	Moving Pictrue Experts Group
OFDM	Orthogonal Frequency Division Multiplexing
PRBS	Pseudo Random Binary Sequence
PIC	Parallel Interference Cancellation
QAM	Quadrature Amplitude Modulation
QoS	Quality of Service
QPSK	Quadrature Phase Shift Keying
SNR	Signal-to-Noise Ratio
SOW	Sliding Observation Window
SP	Serial-to-Parallel
TMMC	Transmission and Multiplexing Configuration Control
VSB	Vestigial Side Band
WiMAX	World Interoperability for Microwave Access
WLAN	Wireless Local Area Network
ZF	Zero-Forcing
ZP	Zero Padded

B. List of Publications

B.1 Journal

1. Z. Ma, M. Okada, "Impulsive Noise Suppression for ISDB-T Receivers Based on Adaptive Window Functions," IEICE Transaction on Fundamentals of Electronics, Communications and Computer Science, Vol.E94-A, No.11, pp 2237 - 2245 , Nov 2011.

2. X. Shao, Z. Ma, "A Novel QoS Source Routing Architecture of Ad Hoc," Computer Applications and Software, Vol.26, No.11, pp 204 - 207, Nov 2009.

B.2 International Conference

1. Z. Ma, T. Sato, M. Okada, "Compressed Sensing Based ICI Cancellation Method for OFDM Systems," ICCE2012, Las Vegas, NV, USA, Jan 2012.

2. Z. Ma, T. Sato, M. Okada and H. Furudate, "ICI Cancellation Method for OFDM Systems using Compressed Sensing Based Channel Estimation," ISPACS2011, ChiangMai, Thailand, Dec 2011.

3. M. Okada, Z. Ma, "Impulse Noise Suppression of OFDM Using Linear Programming," ISCIT2011, Hangzhou, China, Oct 2011.

4. Z. Ma, R. Miyamoto, M. Okada, "Adaptive Impulsive Noise Suppression for ISDB-T Receivers," International Conference on Signal and Information Processing (ICSIP2010), Changsha, China, Dec 2010.

5. Z. Ma, R. Miyamoto, M. Okada, "An Adaptive Scheme of Impulsive Noise Suppression for ISDB-T Receivers," ISPACS 2010, Chengdu, China, Dec 2010.

6. Z. Ma, R. Miyamoto, M. Okada, "An Impulsive Noise Suppression Scheme for an ISDB-T Receivers using Adaptive Parameter Estimation," International Workshop on Smart Info-Media Systems in Asia (SISA 2010), Manilla, Philippine, Sep 2010.

C. Derivation of T_{imp}

In this appendix, we show the derivation of Eq(4.5). From BER vs CNR curves with varying threshold multiplying factors T_v, we choose the T_v with optimum BER performance among them. The relation between the optimum threshold multiplying factor T_v and CNR is shown in Fig. C.1. Observing the distribution of T_v, we can use a quadratic polynomial function to fit the discrete data points. The value of T_v and CNR is only set in integer. But from the results of simulation experiments, the assumed function curve practically comes close to fitting the threshold levels with sub-optimum performance. Therefore we adopt Eq(4.5) as the threshold function of T_{imp}.

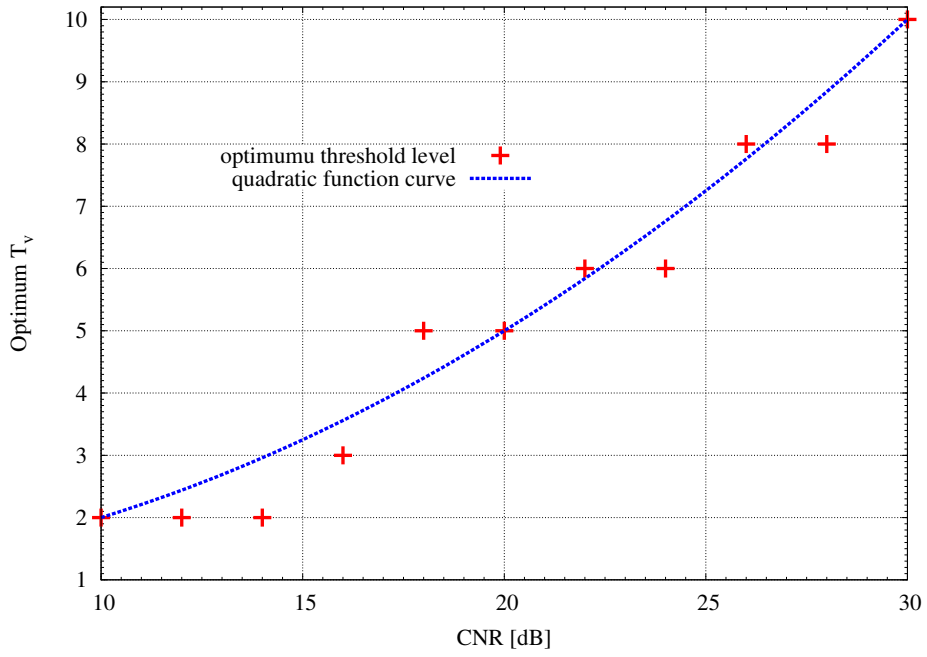

Figure C.1. CNR vs optimum T_v, curve fitting between the proposed method and simulation data.